Anion recognition and transport properties of sulfamide-, phosphoric triamide- and thiophosphoric triamide-based receptors

Philippa B. Cranwell,[a] Jennifer R. Hiscock,[a] Cally J.E. Haynes,[a] Mark E. Light,[a] Neil J. Wells[a] and Philip A. Gale[a*]

Electronic Supplementary Information

Experimental

General remarks: All reactions were performed under slight positive pressure of nitrogen using oven dried glassware. ^{1}H NMR (300 MHz) and ^{1}H NMR (400 MHz) were determined on a Bruker AV300 and AV400 spectrometer respectively with the chemical shifts reported in parts per million (ppm), calibrated to the centre of the solvent peak set. All solvents and starting materials were purchased from chemical stores where available. NMR titrations were performed by adding aliquots of the putative anionic guest (as the tetrabutylammonium/TBA salt or tetraethylammonium/TEA salt in the case of bicarbonate) (0.15 M) in a solution of the receptor (0.1 M) in a DMSO-d_6/0.H_2O 0.5 % mixture to a solution of the receptor (0.01 M). Job plots we performed by analysis of mixtures of two DMSO-d_6/H_2O 0.5% solutions, receptor (0.01 M) and putative anionic guest (TBA/TEA salt) (0.01 M) in various ratios. U-tube protocol - Source phase: 489 mM NaCl buffered to pH 7.2 with 5 mM sodium phosphate salts, 10 mL. Receiver phase: 489 mM NaNO3 buffered to pH 7.2 with 5 mM sodium phosphate salts, 10 mL. Organic phase: 1 mM tetrabutylammonium hexafluorophosphate in nitrobenzene with 1 mM receptor (no receptor was added for comparative blank run), 20 mL. The organic phase was stirred gently at room temperature, and the chloride concentration of the receiver phase was determined using a chloride sensitive electrode at set intervals.

Bis(3,5-bis(trifluoromethyl)phenyl) sulfamide (1) To 3,5-bis(trifluoromethyl)aniline (1.99 mL, 12.8 mmol) in CH_2Cl_2 (35 mL) at 0 ºC was added freshly distilled triethylamine (3.6 mL, 25.6 mmol) followed by sulfuryl chloride (519 µL, 6.4 mmol) dropwise. The reaction was heated to reflux overnight to give an orange solution. The reaction was diluted with CH_2Cl_2 (50 mL), washed with sat. aq. NH_4Cl (3 × 100 mL) and the organic phase washed with brine (100 mL), dried ($MgSO_4$) and the solvent removed *in vacuo*. Purification by flash column chromatography (5% EtOAc/Hexane) furnished the target compound (634 mg, 1.22 mmol, 19%) as a pale yellow solid. Spectra consistent with reported data.[1]

Tris(3,5-bis(trifluoromethyl)phenyl) phosphotriamide (2) To 3,5-bis(trifluoromethyl)aniline (1 mL, 6.4 mmol) in freshly distilled triethylamine (2.7 mL, 19.2 mmol) at 0 ºC was added phosphorous(V) oxychloride (179 µL, 1.9 mmol) dropwise. The reaction was heated to reflux for 16 hours to give a red solid. The solid was dissolved CH_2Cl_2 (50 mL), washed with sat. aq. NH_4Cl (3 × 100 mL) and the organic phase washed with brine (100 mL), dried ($MgSO_4$) and the solvent removed *in vacuo*. Purification by flash column chromatography (10% EtOAc/Hexane) furnished the target compound. (304 mg, 0.42 mmol, 22%) as a pale yellow solid. Spectra consistent with reported data.[1]

Tris(3,5-bis(trifluoromethyl)phenyl) thiophosphotriamide (3) To 3,5-bis(trifluoromethyl)aniline (1 mL, 6.4 mmol) in freshly distilled triethylamine (4 mL, 28.6 mmol) at 0 ºC was added thiophosphoryl chloride (195 µL, 1.9 mmol) dropwise to give a cloudy suspension. The reaction was heated to reflux for 16 hours. The reaction was diluted with CH_2Cl_2 (50 mL), washed with sat. aq. NH_4Cl (3 × 100 mL) and the organic phase washed with brine (100 mL), dried ($MgSO_4$) and the solvent removed *in vacuo*. Purification by flash column

chromatography (5% EtOAc/Hexane) furnished the target compound (316 mg, 0.42 mmol, 22%) as a pale yellow solid. Spectra consistent with reported data.[1]

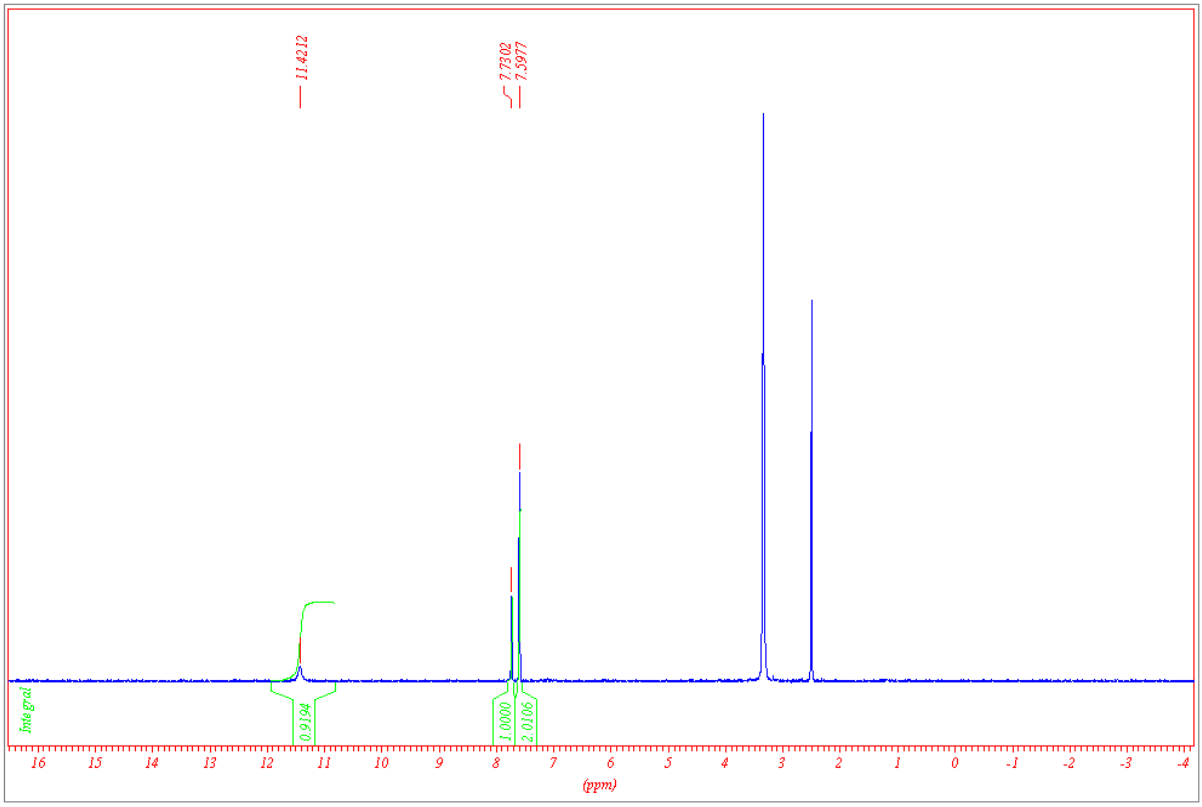

Figure S1 ^{1}H NMR spectrum of compound **1** in DMSO-d_6.

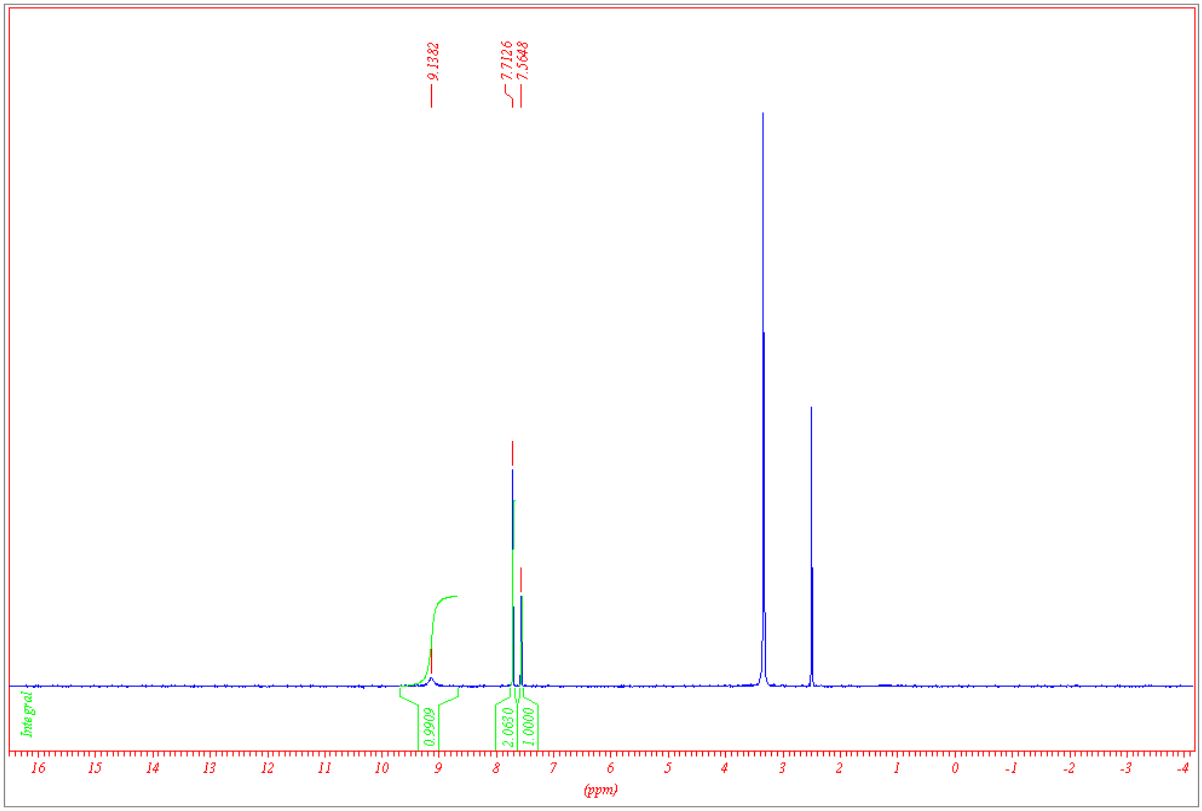

Figure S2 ^{1}H NMR spectrum of compound **2** in DMSO-d_6.

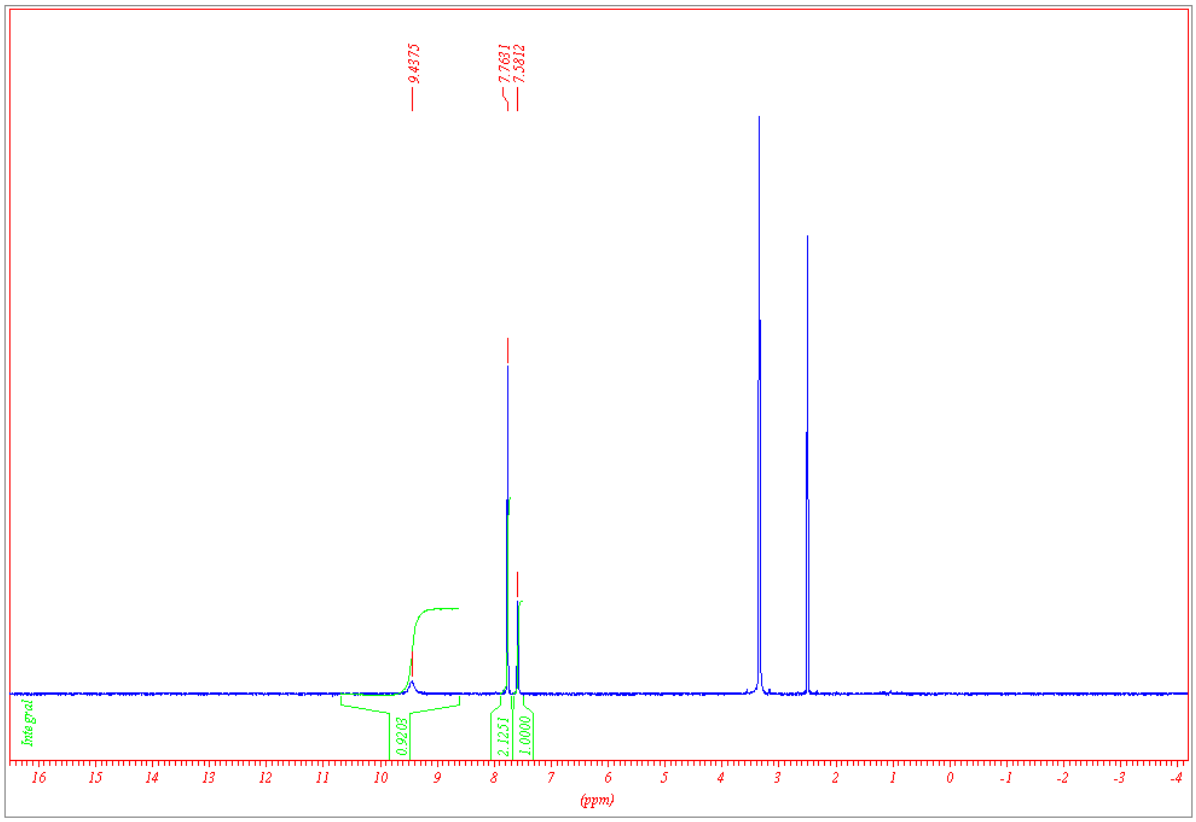

Figure S3 ^{1}H NMR spectrum of compound **3** in DMSO-d_6.

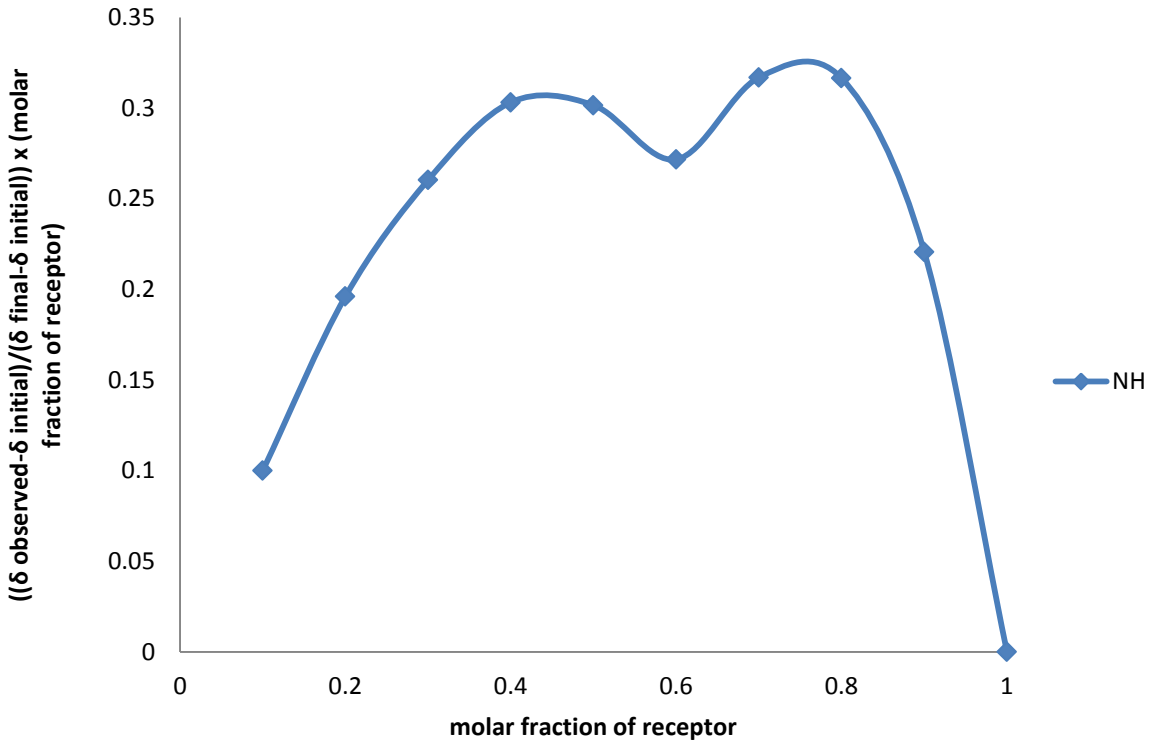

Figure S4 ^{1}H NMR determined Job plot of compound **2** *vs.* TBACl in DMSO-d_6/H_2O 0.5 %.

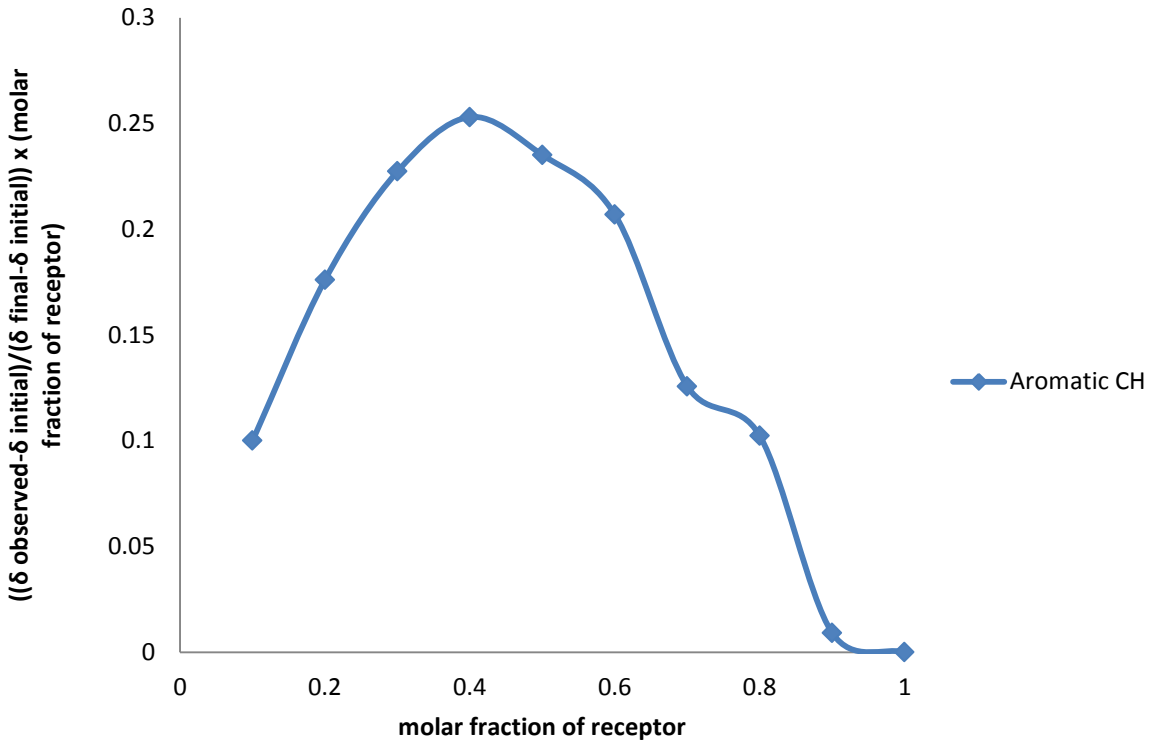

Figure S5 ^{1}H NMR determined Job plot of compound **2** *vs.* $TBAH_2PO_4$ in DMSO-d_6/H_2O 0.5 %.

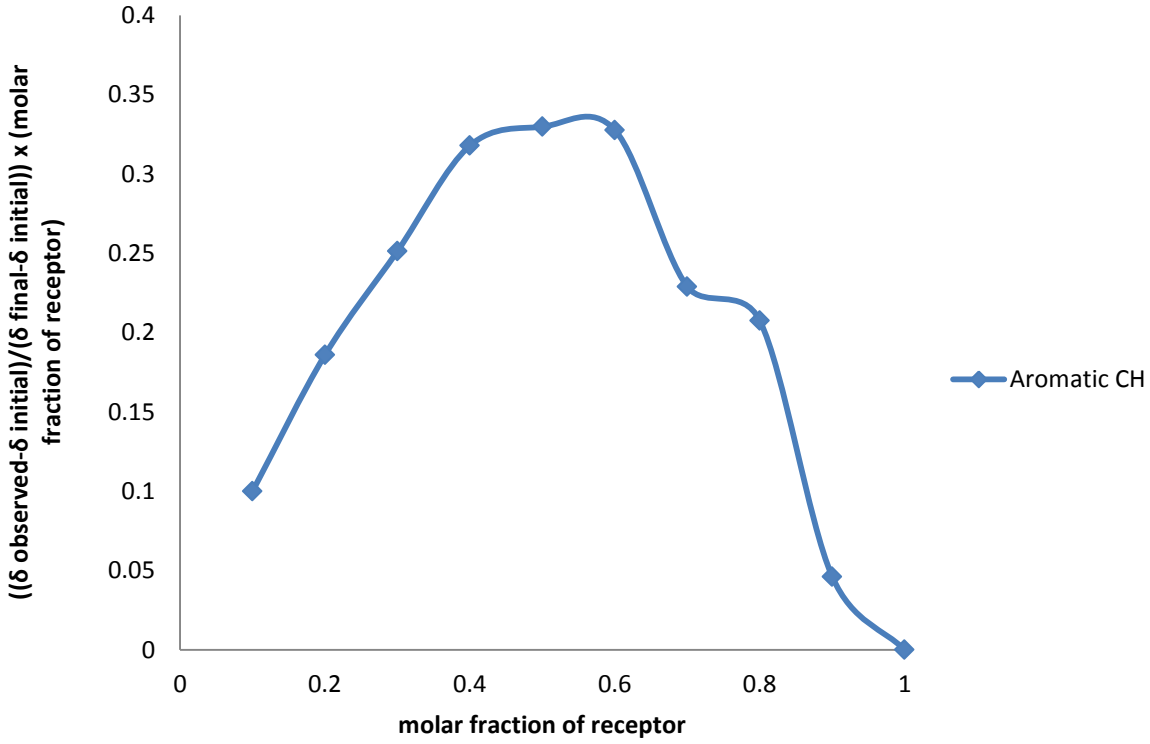

Figure S6 ^{1}H NMR determined Job plot of compound **2** *vs.* TBAOAc in DMSO-d_6/H_2O 0.5 %.

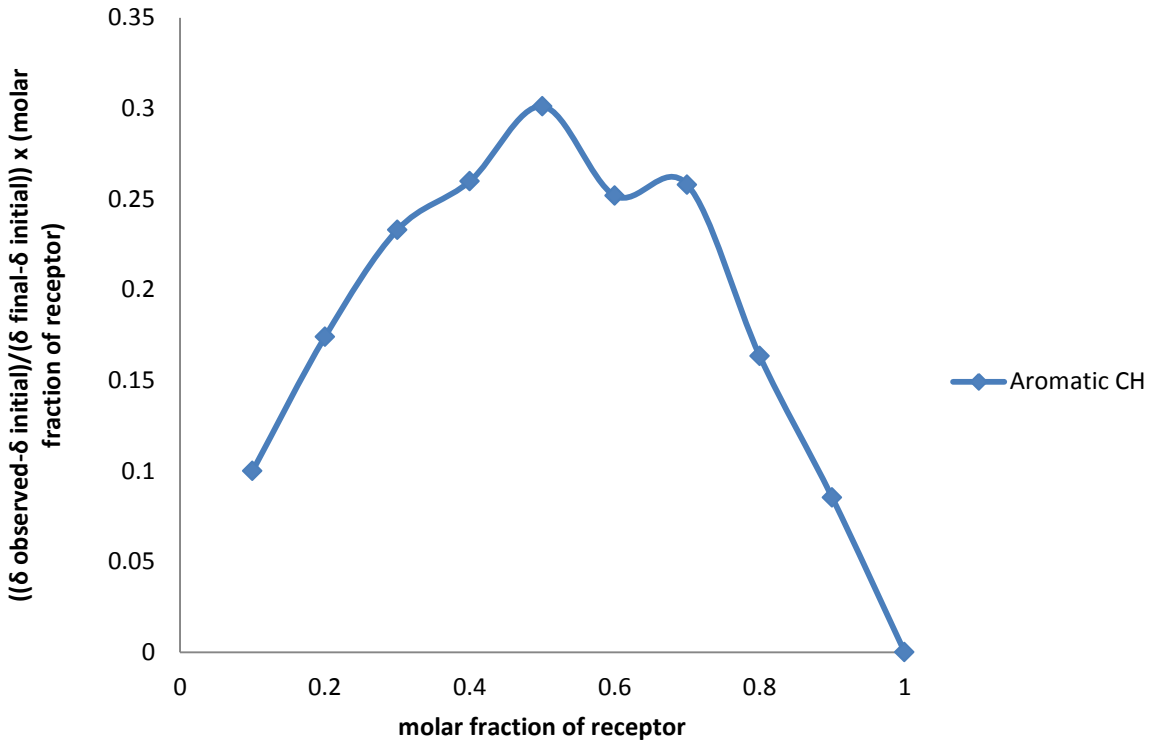

Figure S7 ^{1}H NMR determined Job plot of compound **2** *vs.* TBAOBz in DMSO-d_6/H_2O 0.5 %.

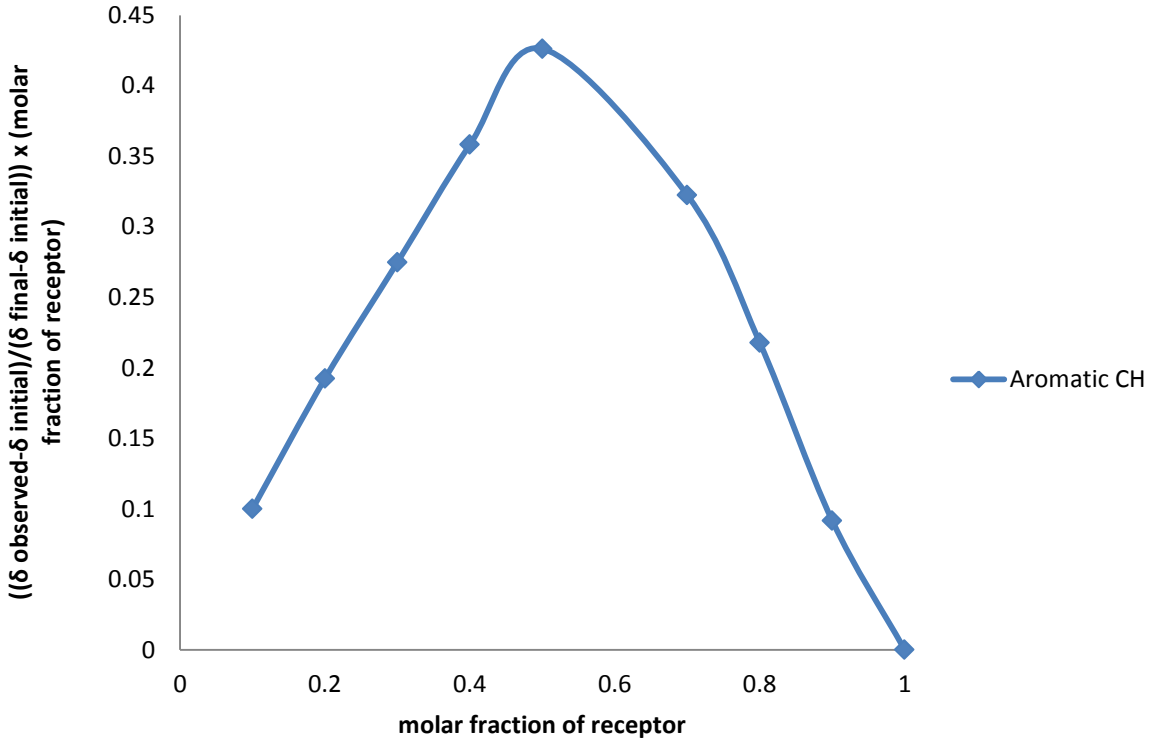

Figure S8 ^{1}H NMR determined Job plot of compound **2** *vs.* TBA_2SO_4 in DMSO-d_6/H_2O 0.5 %.

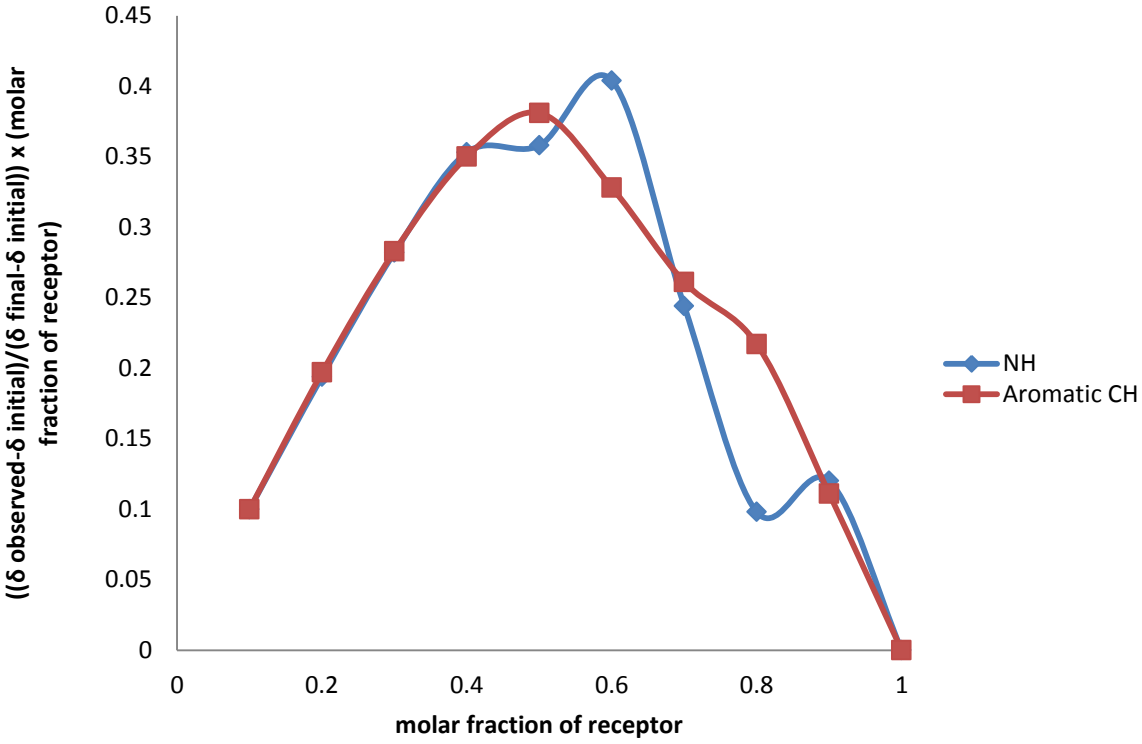

Figure S9 ^{1}H NMR determined Job plot of compound **3** *vs.* TBABr in MeCN-d_3.

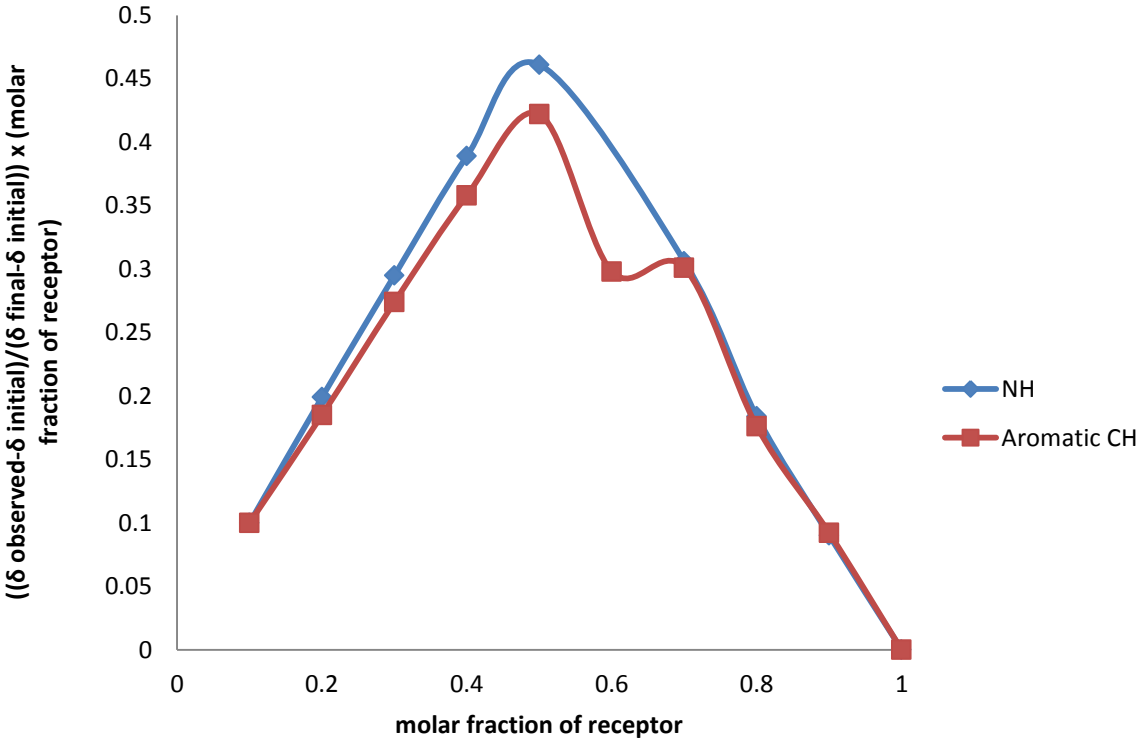

Figure S10 ^{1}H NMR determined Job plot of compound **3** *vs.* TBACl in MeCN-d_3.

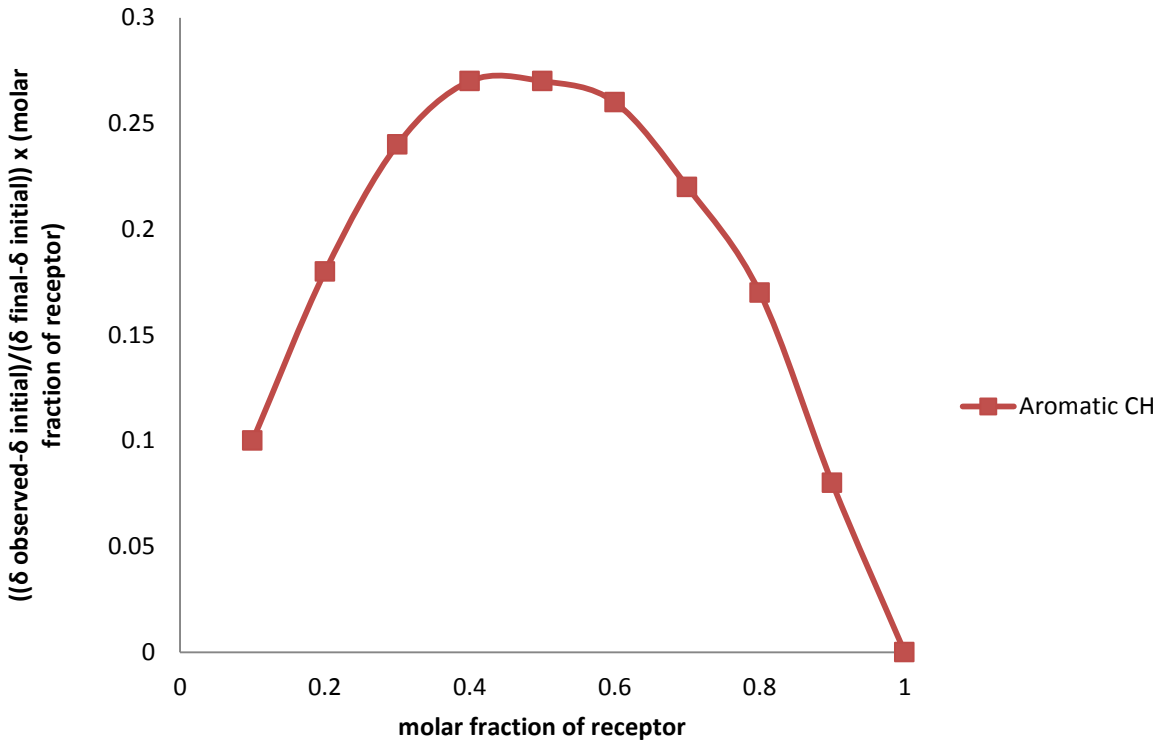

Figure S11 ^{1}H NMR determined Job plot of compound **3** *vs.* TBAI in MeCN-d_3.

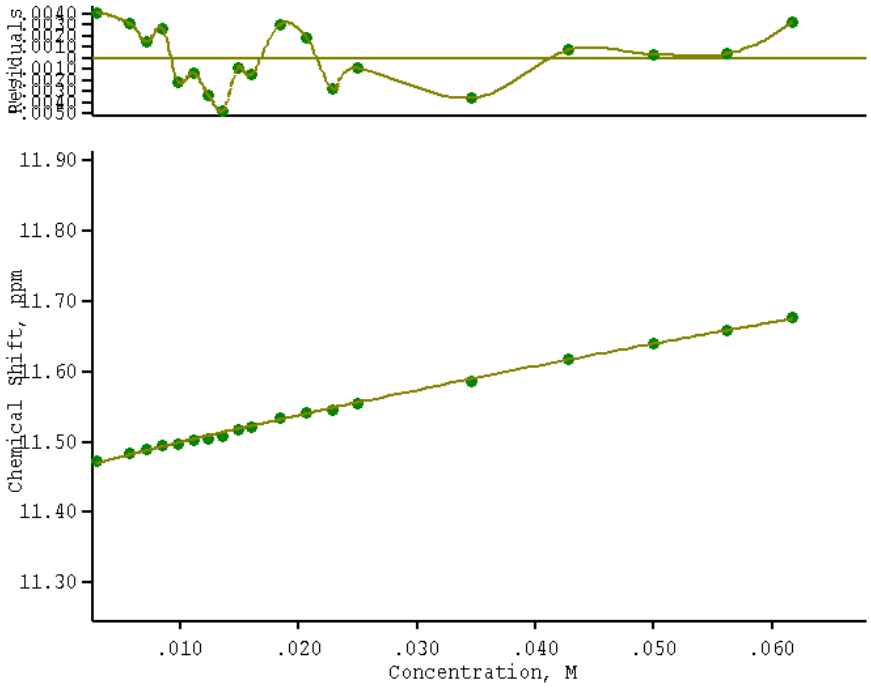

K_1 = <10 M^{-1} Error = NA

Figure S12 ^{1}H NMR titration of compound **1** *vs.* TBACl in DMSO-d_6/H_2O 0.5%. Following the NH.

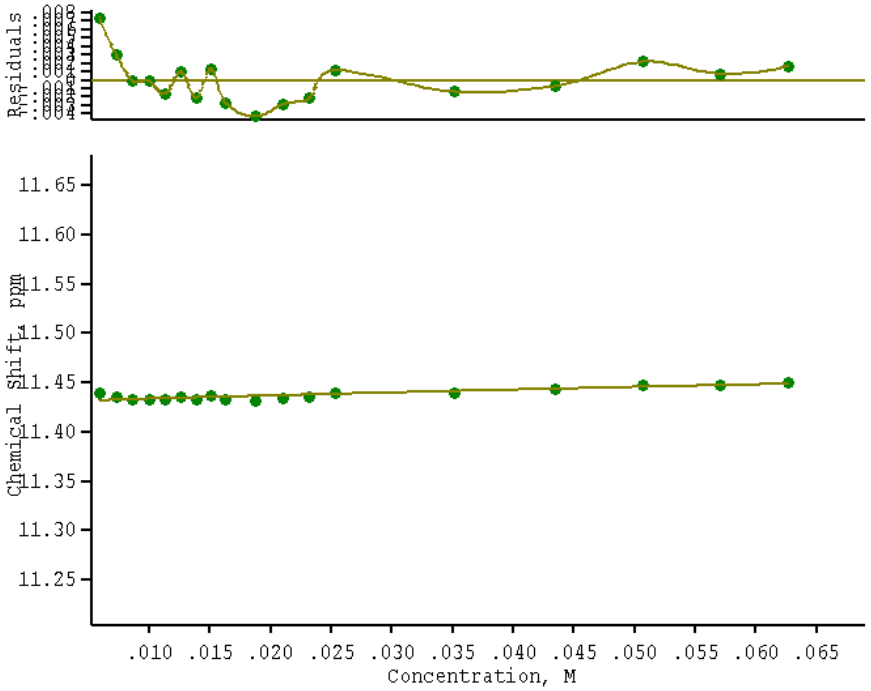

K_1 = <10 M^{-1} Error = NA

Figure S13 ^{1}H NMR titration of compound **1** *vs.* TBABr in DMSO-d_6/H_2O 0.5%. Following the NH.

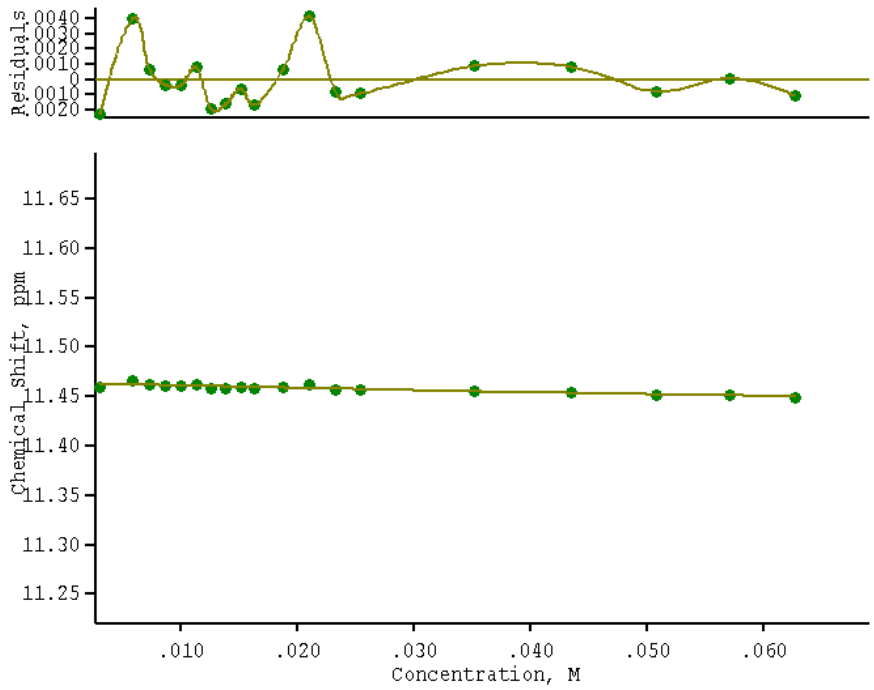

K_1 = <10 M^{-1} Error = NA

Figure S14 ^{1}H NMR titration of compound **1** *vs.* TBAI in DMSO-d_6/H_2O 0.5%. Following the NH.

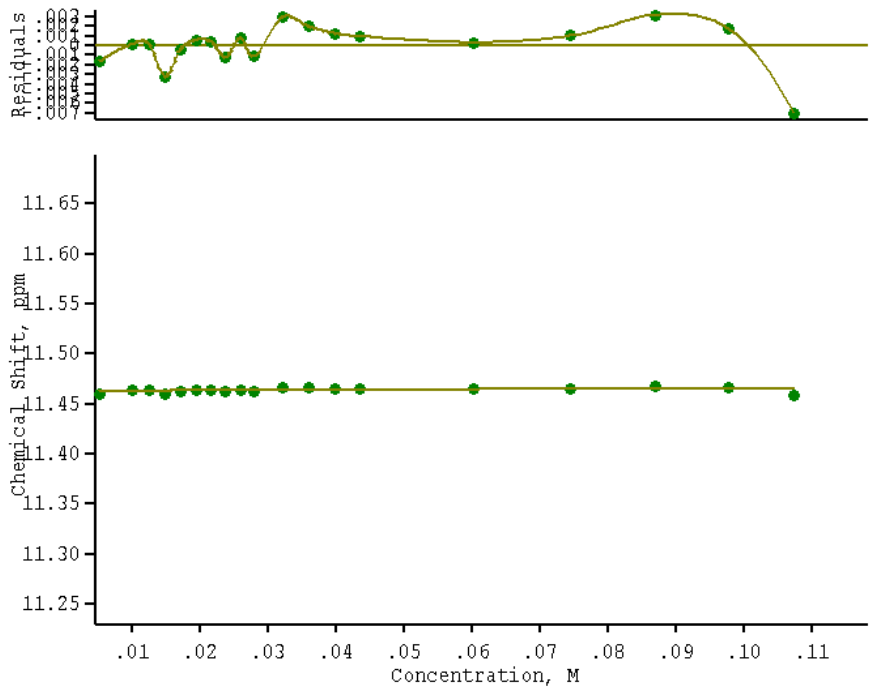

K_1 = <10 M^{-1} Error = NA

Figure S15 ^{1}H NMR titration of compound **1** *vs.* $TBAHSO_4$ in DMSO-d_6/H_2O 0.5%. Following the NH.

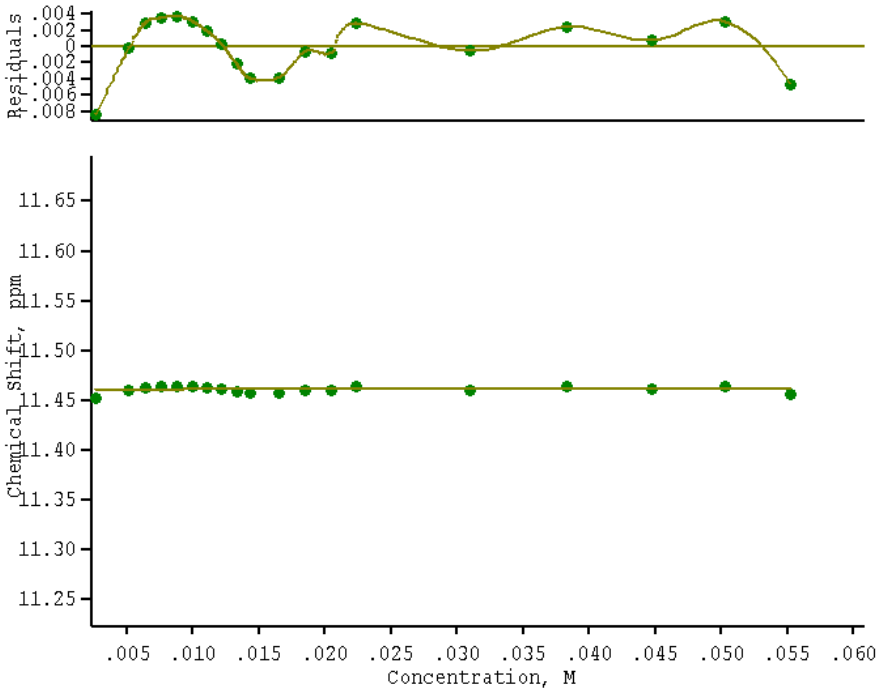

K_1 = <10 M^{-1} Error = NA

Figure S16 ^{1}H NMR titration of compound **1** *vs.* $TBANO_3$ in DMSO-d_6/H_2O 0.5%. Following the NH.

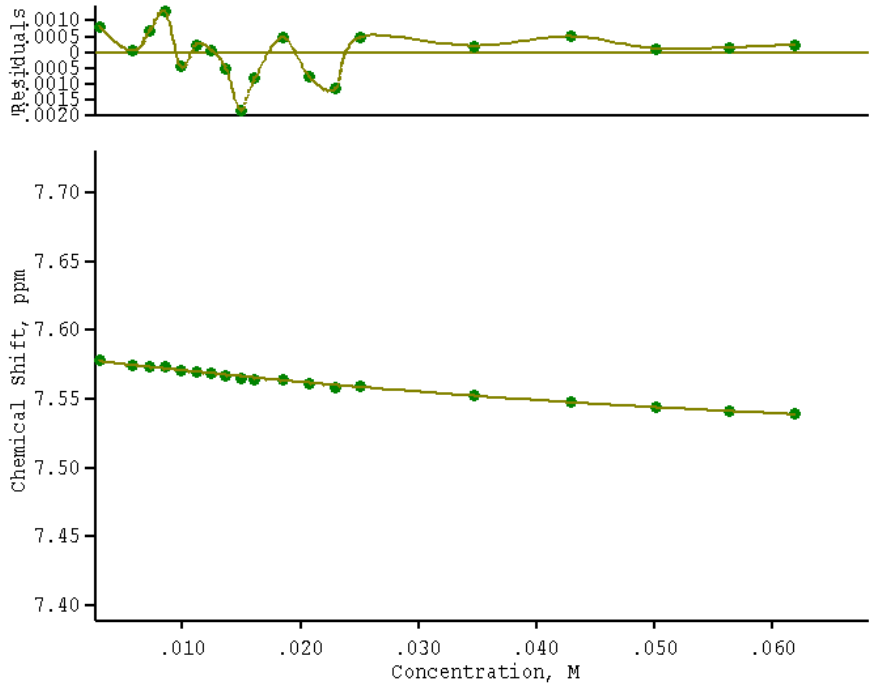

K_1 = 13 M^{-1} Error = ± 7 %

Figure S17 ^{1}H NMR titration of compound **2** *vs.* TBACl in DMSO-d_6/H_2O 0.5%. Following the aromatic CH.

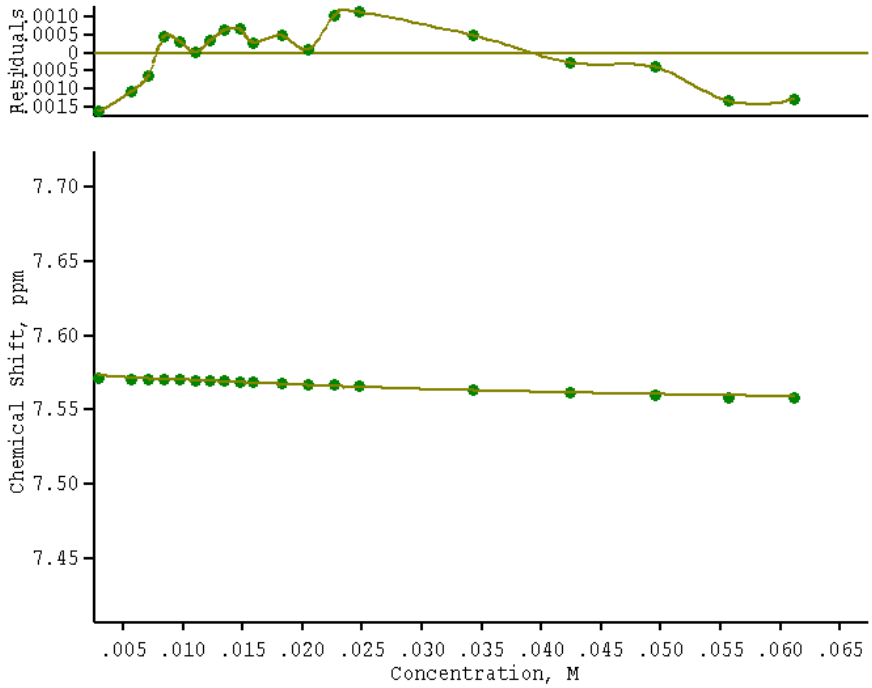

K_1 = 32 M^{-1} Error = ± 6 %

Figure S18 ^{1}H NMR titration of compound **2** *vs.* TBABr in DMSO-d_6/H_2O 0.5%. Following the aromatic CH.

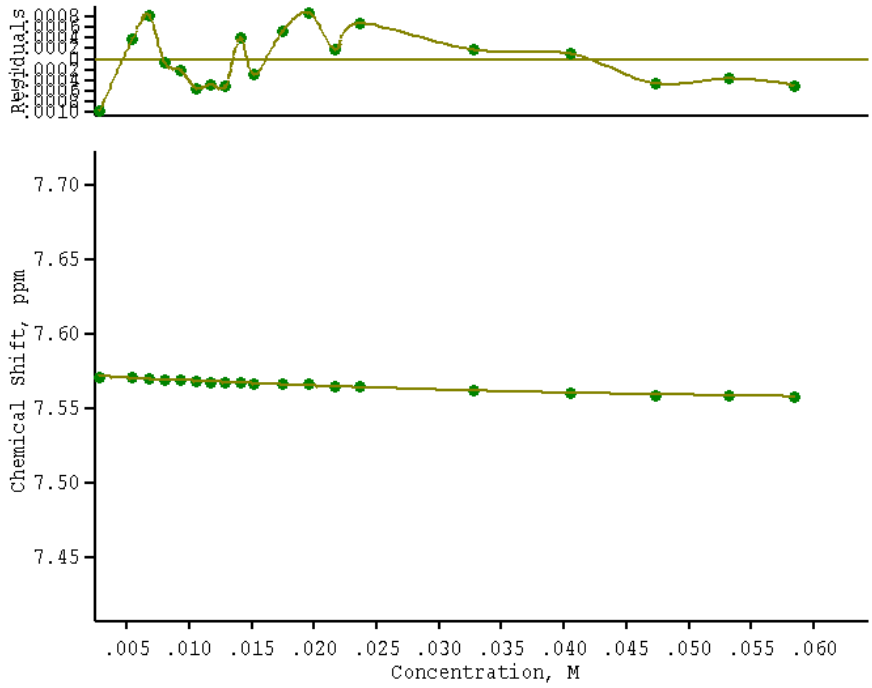

K_1 = 36 M^{-1} Error = ± 6 %

Figure S19 ^{1}H NMR titration of compound **2** *vs.* TBAI in DMSO-d_6/H_2O 0.5%. Following the aromatic CH.

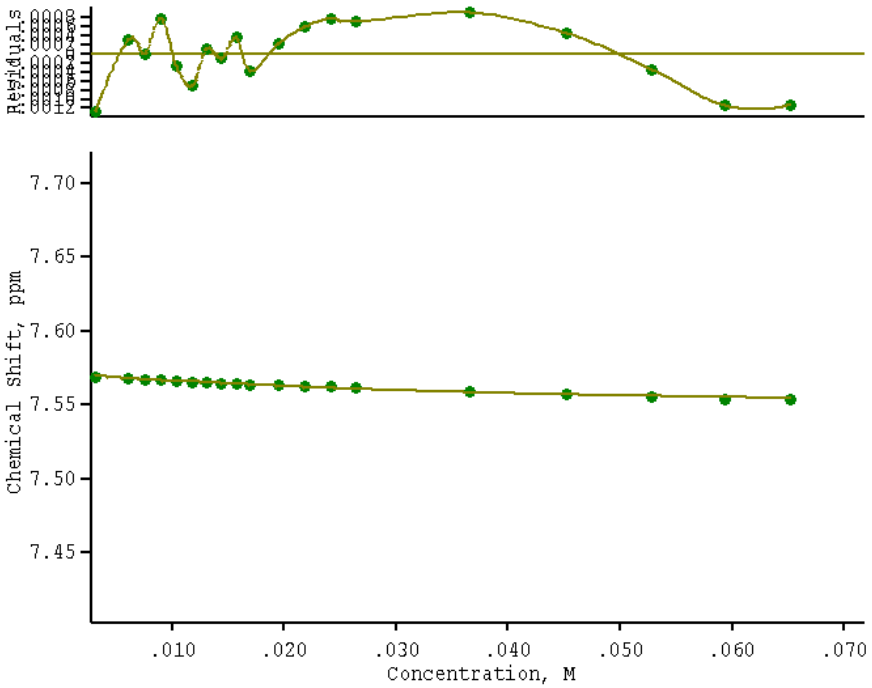

K_1 = 43 M^{-1} Error = ± 4 %

Figure S20 ^{1}H NMR titration of compound **2** *vs.* $TBAHSO_4$ in DMSO-d_6/H_2O 0.5%. Following the aromatic CH.

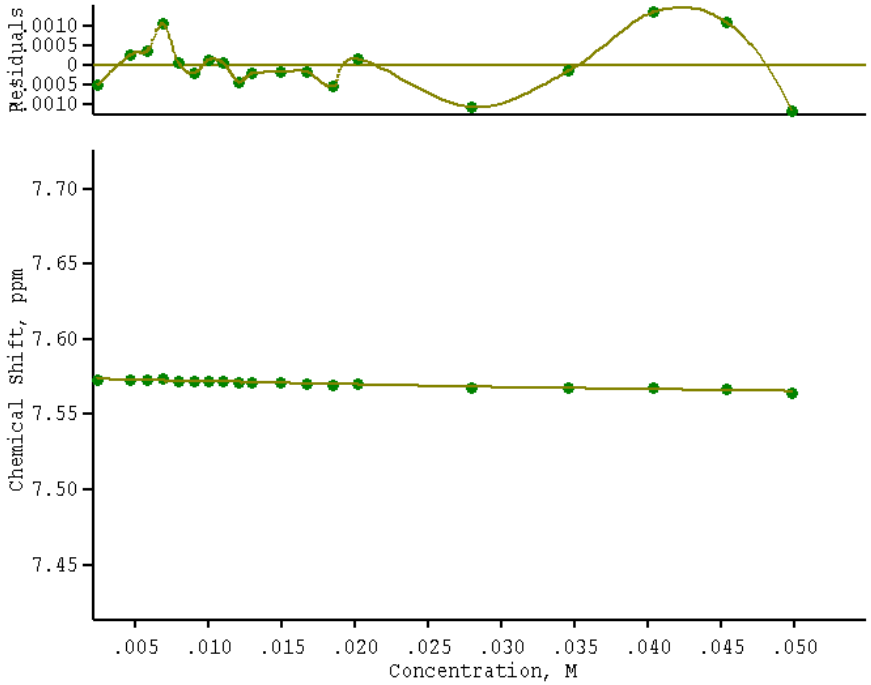

K_1 = 20 M^{-1} Error = ± 7 %

Figure S21 ^{1}H NMR titration of compound **2** *vs.* TBABr in DMSO-d_6/H_2O 0.5%. Following the aromatic CH.

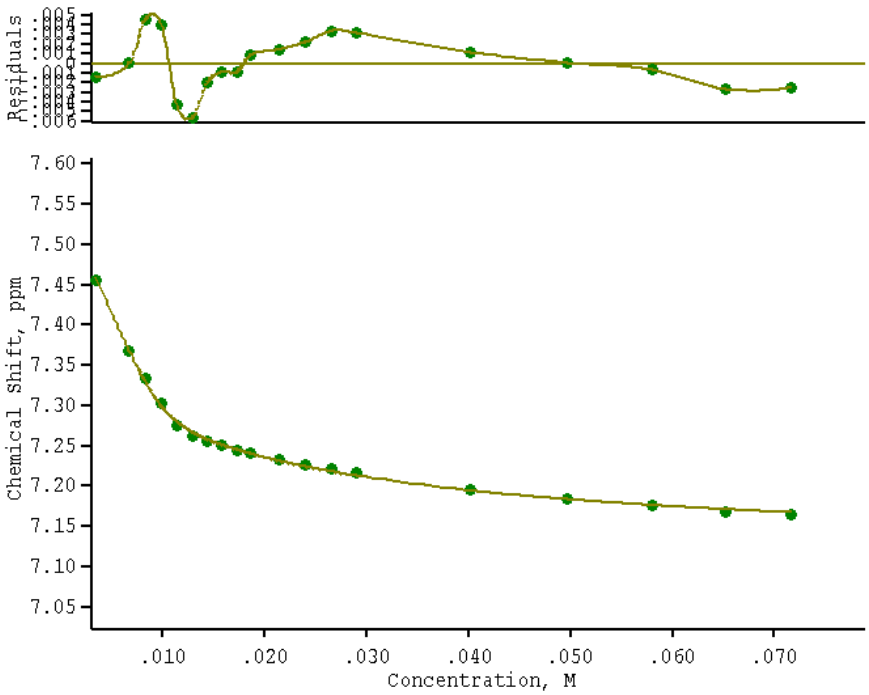

K_1 = 6509 M^{-1} Error = ± 4 %
K_2 = 39 M^{-1} Error = ± 4 %

Figure S22 ^{1}H NMR titration of compound **2** *vs.* TBAOAc in DMSO-d_6/H_2O 0.5%. Following the aromatic CH.

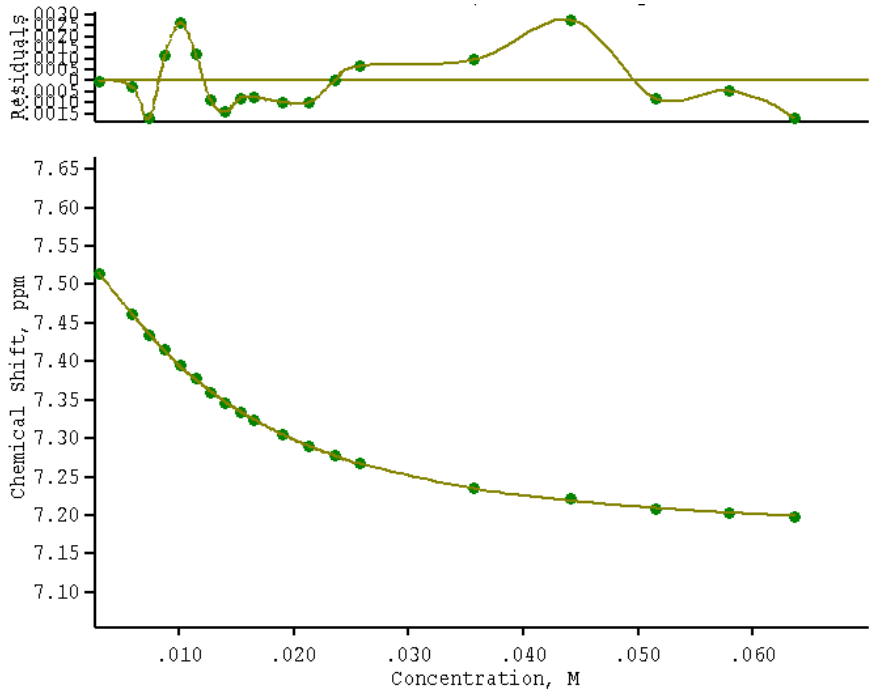

K_1 = 5458 M^{-1} Error = ± 3 %
K_2 = 107 M^{-1} Error = ± 3 %

Figure S23 ^{1}H NMR titration of compound **2** *vs.* $TBAH_2PO_4$ in DMSO-d_6/H_2O 0.5%. Following the aromatic CH.

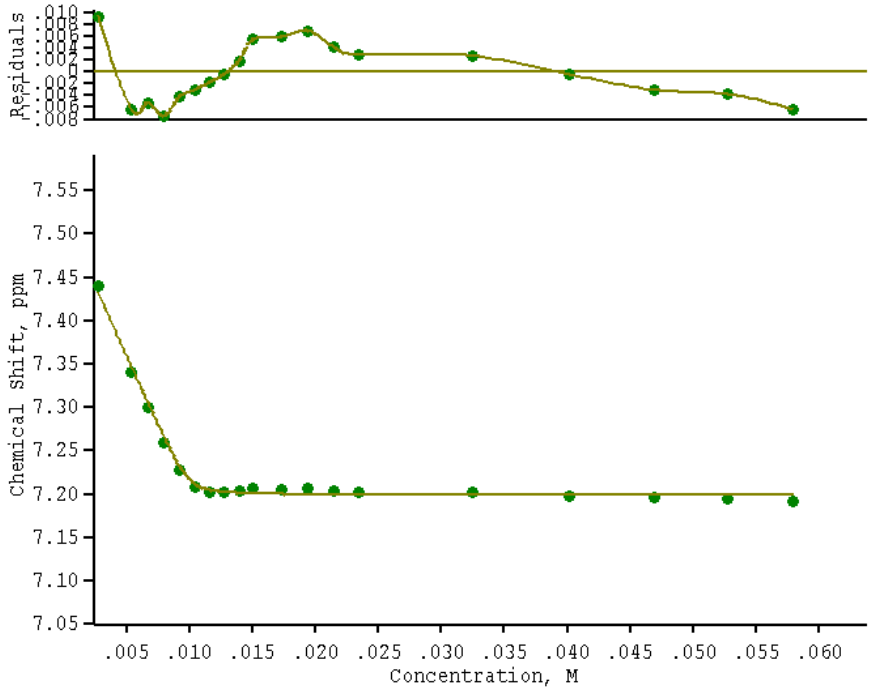

K_1 = > 10^4 M^{-1} Error = NA

Figure S24 ^{1}H NMR titration of compound **2** *vs.* TBA_2SO_4 in DMSO-d_6/H_2O 0.5%. Following the aromatic CH.

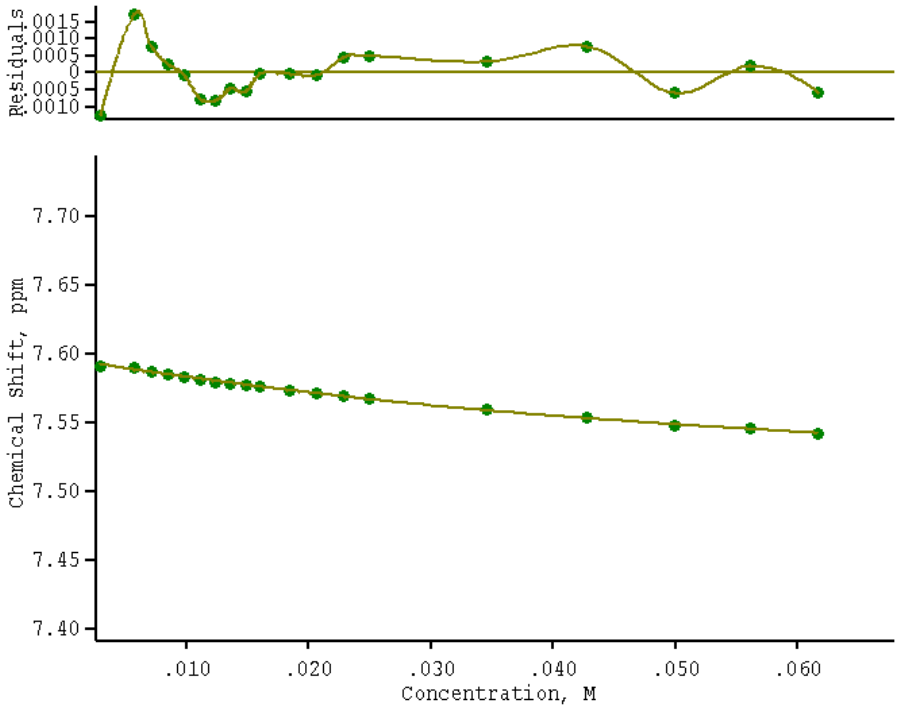

K_1 = 17 M^{-1} Error = ± 7 %

Figure S25 ^{1}H NMR titration of compound **3** *vs.* TBACl in DMSO-d_6/H_2O 0.5%. Following the aromatic CH.

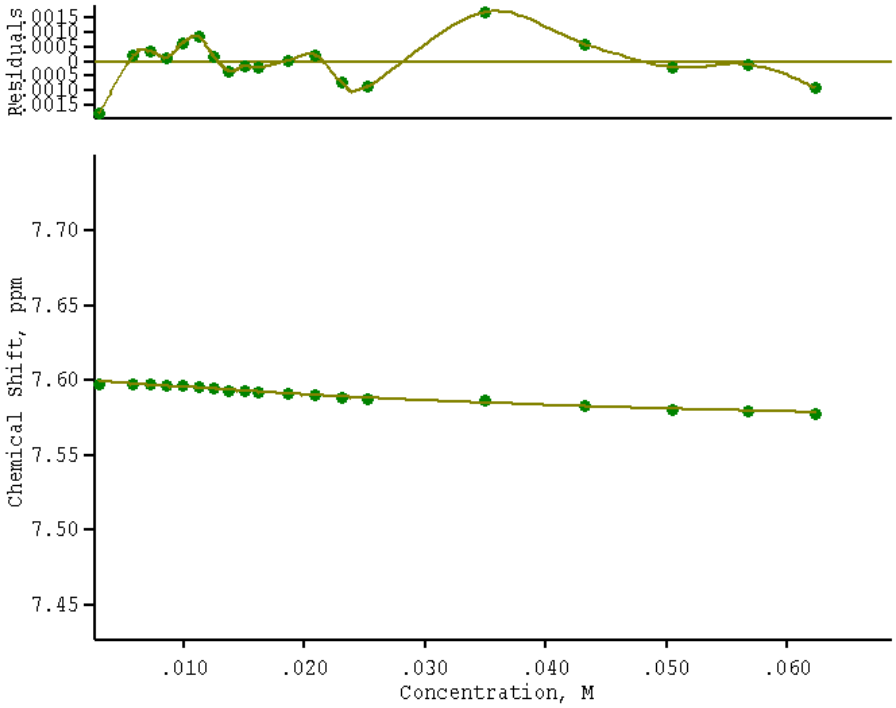

K_1 = 25 M^{-1} Error = ± 6 %

Figure S26 ^{1}H NMR titration of compound **3** *vs.* TBABr in DMSO-d_6/H_2O 0.5%. Following the aromatic CH.

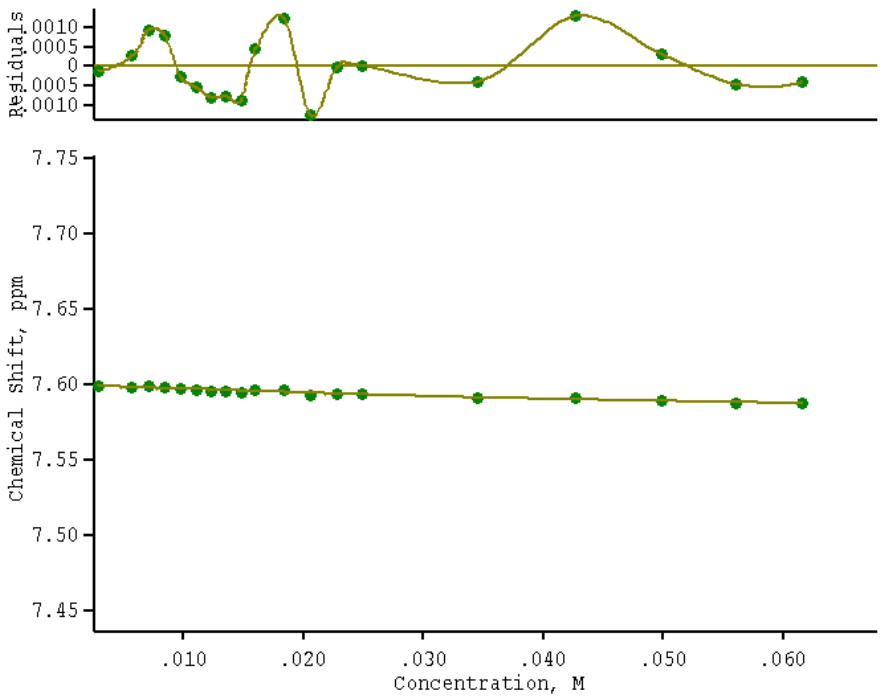

K_1 = 21 M^{-1} Error = ± 6 %

Figure S27 ^{1}H NMR titration of compound **3** *vs.* TBAI in DMSO-d_6/H_2O 0.5%. Following the aromatic CH.

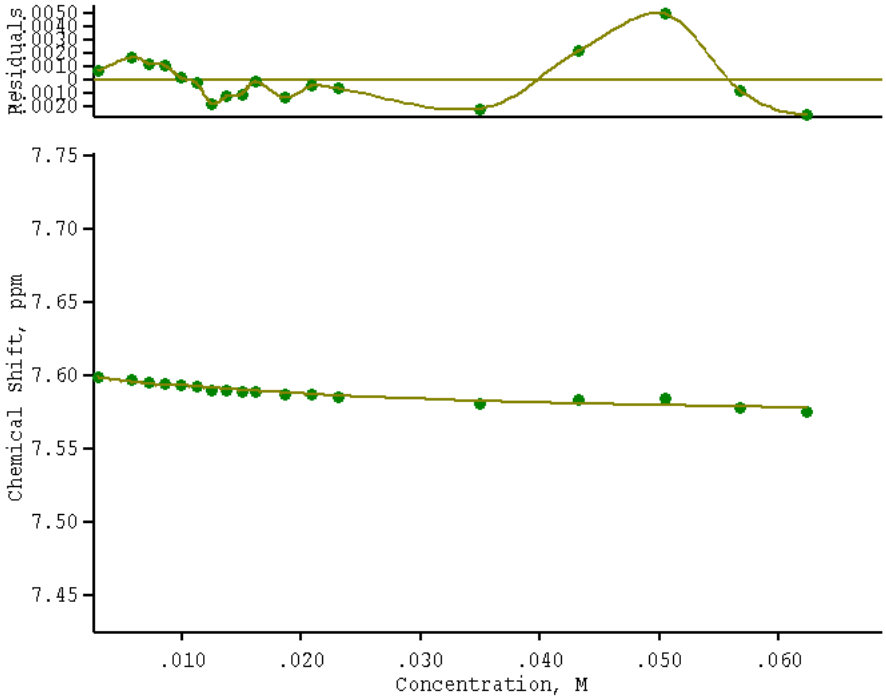

K_1 = 57 M^{-1} Error = ± 6 %

Figure S28 ^{1}H NMR titration of compound **3** *vs.* $TBAHSO_4$ in DMSO-d_6/H_2O 0.5%. Following the aromatic CH.

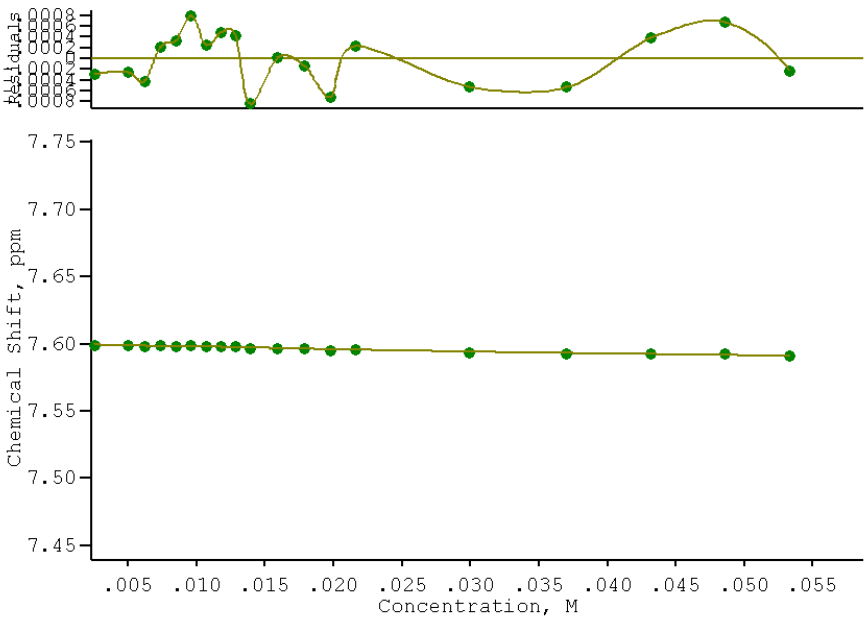

K_1 = 16 M^{-1} Error = ± 10 %

Figure S29 ^{1}H NMR titration of compound **3** *vs.* $TBANO_3$ in DMSO-d_6/H_2O 0.5%. Following the aromatic CH.

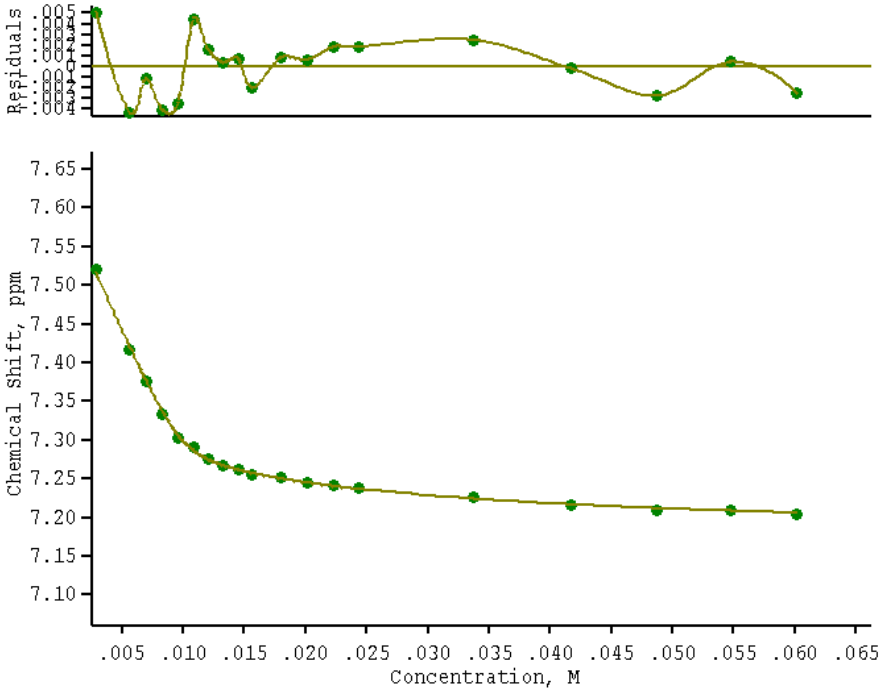

K_1 = 10034 M^{-1} Error = ± 3 %
K_2 = 48 M^{-1} Error = ± 3 %

Figure S30 ^{1}H NMR titration of compound **3** *vs.* TBAOBz in DMSO-d_6/H_2O 0.5%. Following the aromatic CH.

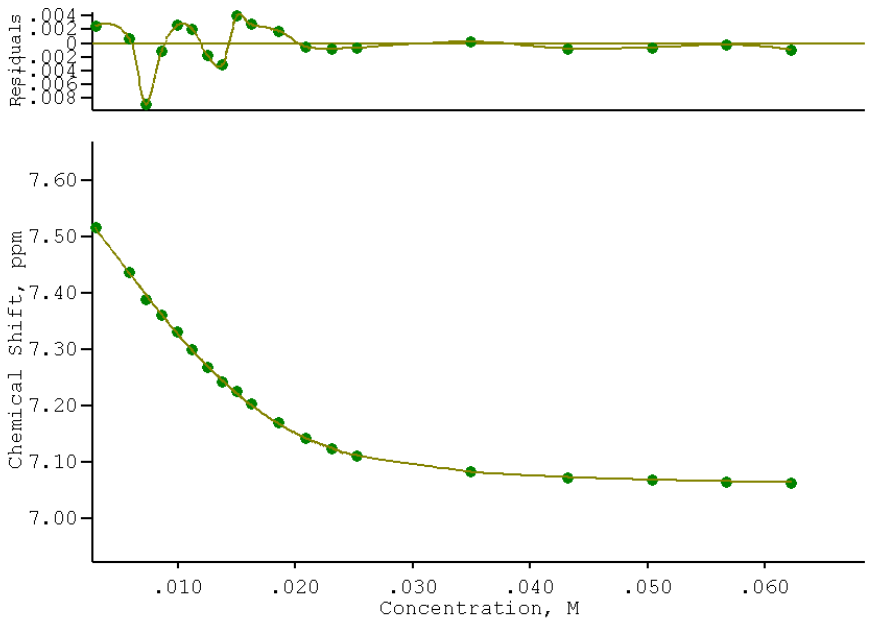

K_1 = 2042 M^{-1} Error = ± 7 %
K_2 = 432 M^{-1} Error = ± 7 %

Figure S31 ^{1}H NMR titration of compound **3** *vs.* $TBAH_2PO_4$ in DMSO-d_6/H_2O 0.5%. Following the aromatic CH.

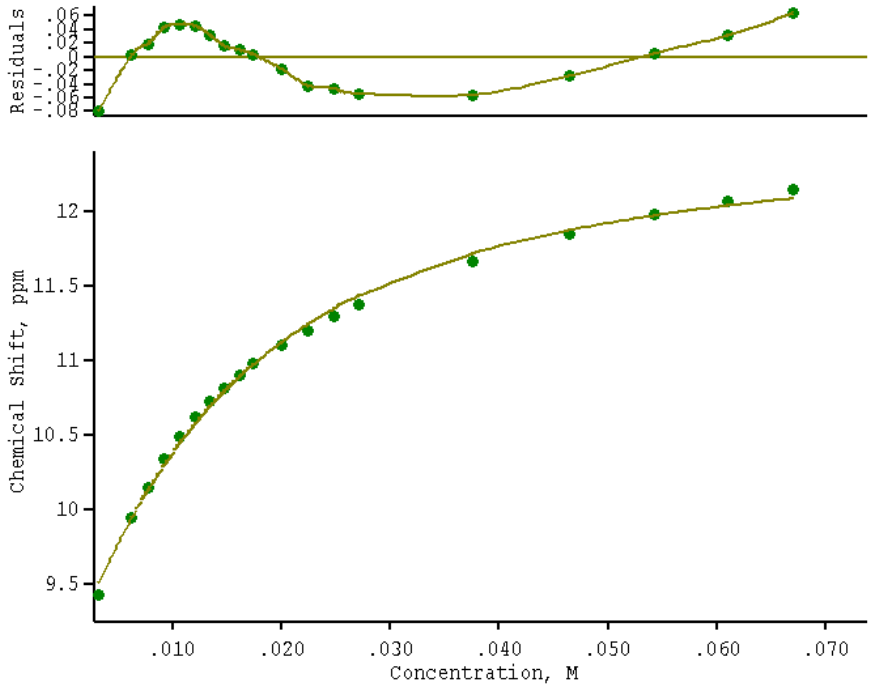

K_1 = 104 M^{-1} Error = ± 8 %

Figure S32 ^{1}H NMR titration of compound **1** *vs.* TBACl in MeCN-d_3. Following the NH.

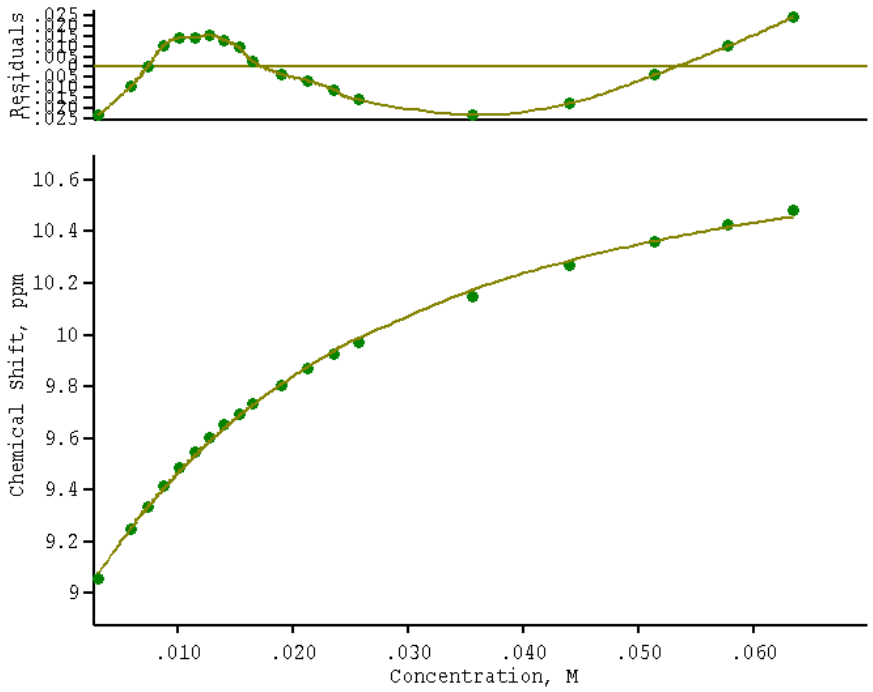

K_1 = 59 M^{-1} Error = ± 6 %

Figure S33 ^{1}H NMR titration of compound **1** *vs.* TBABr in MeCN-d_3. Following the NH.

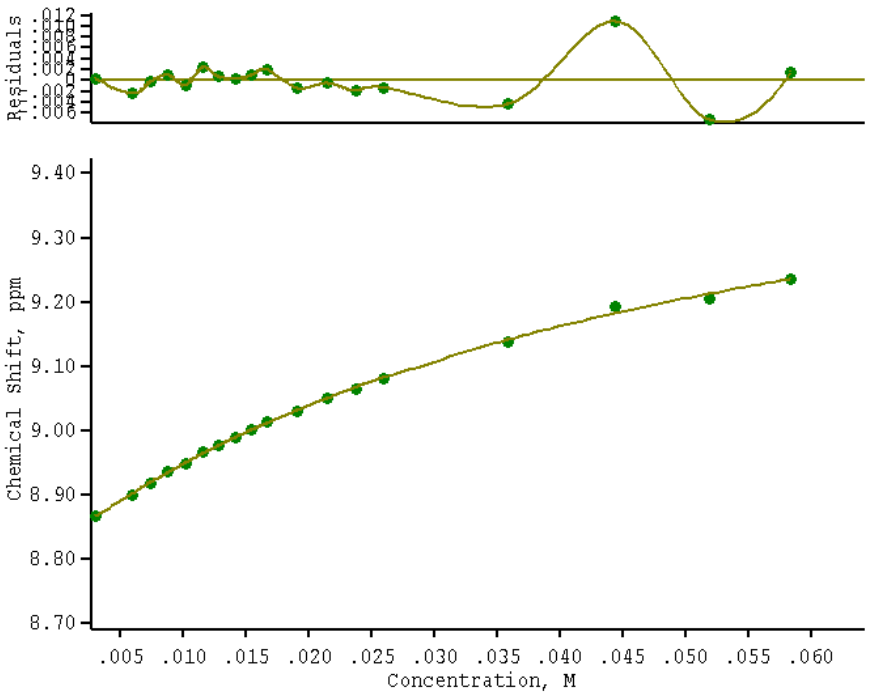

K_1 = 25 M^{-1} Error = ± 7 %

Figure S34 ^{1}H NMR titration of compound **1** *vs.* TBAI in MeCN-d_3. Following the NH.

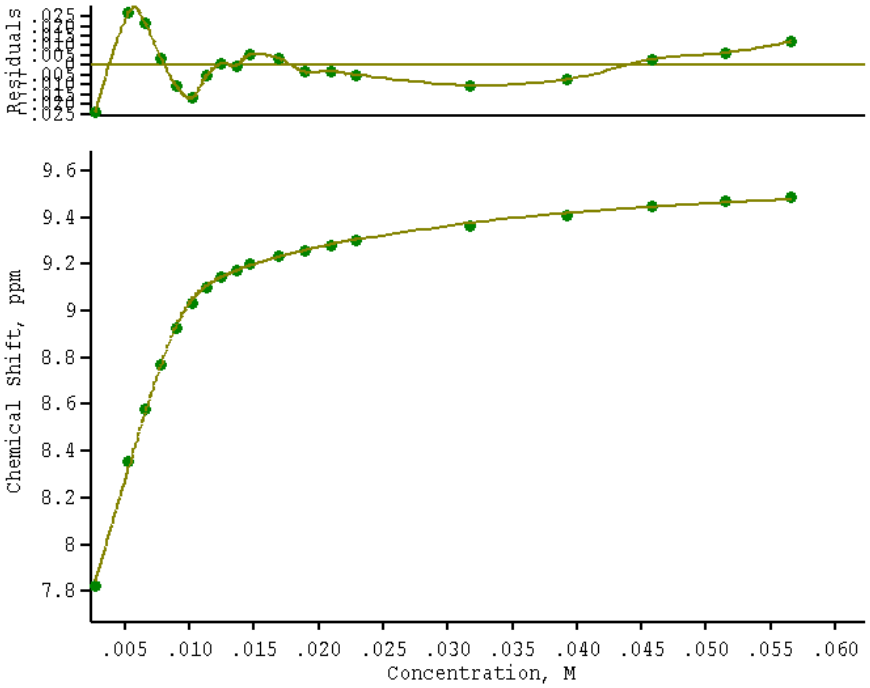

K_1 = 17374 M^{-1} Error = ± 5 %
K_2 = 59 M^{-1} Error = ± 5 %

Figure S35 ^{1}H NMR titration of compound **2** *vs.* TBACl in MeCN-d_3. Following the NH.

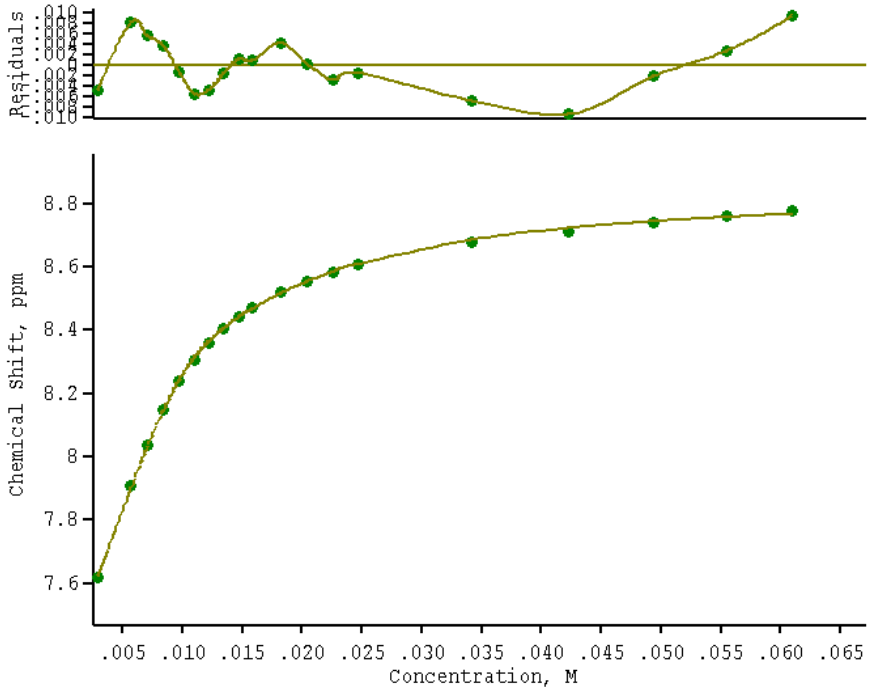

K_1 = 10781 M^{-1} Error = ± 3 %
K_2 = 120 M^{-1} Error = ± 5 %

Figure S36 ^{1}H NMR titration of compound **2** *vs.* TBABr in MeCN-d_3. Following the NH.

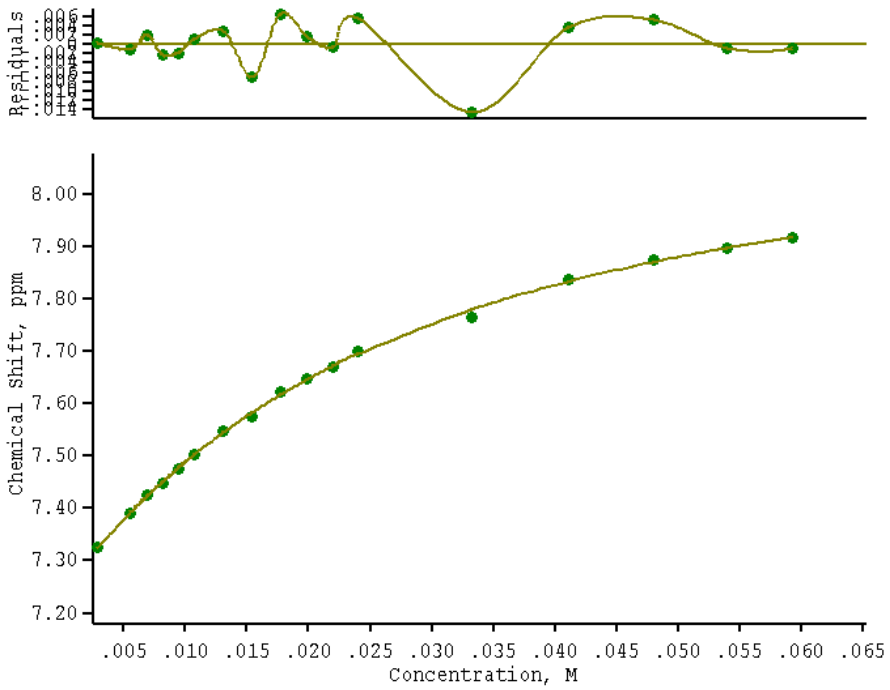

K_1 = 48 M^{-1} Error = ± 5 %

Figure S37 ^{1}H NMR titration of compound **2** *vs.* TBAI in MeCN-d_3. Following the NH.

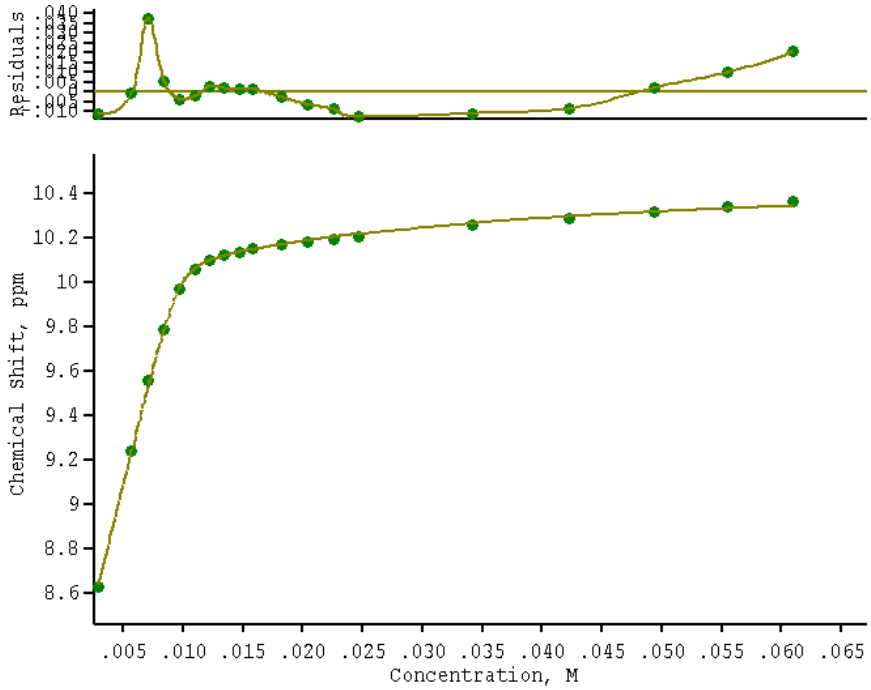

K_1 = 26751 M^{-1} Error = ± 4 %
K_2 = 36 M^{-1} Error = ± 4 %

Figure S38 ^{1}H NMR titration of compound **3** *vs.* TBACl in MeCN-d_3. Following the NH.

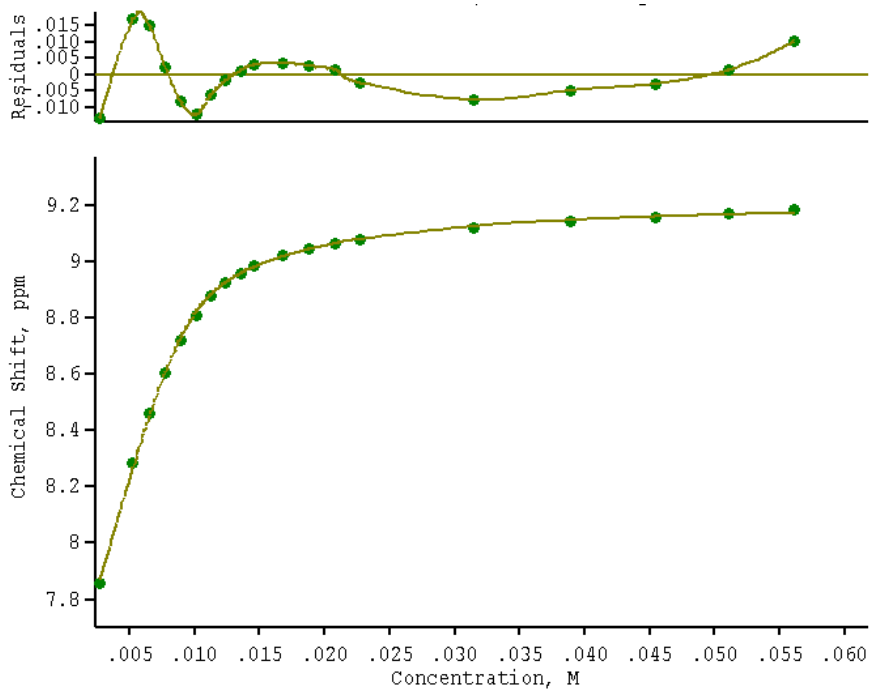

K_1 = 8506 M^{-1} Error = ± 5 %
K_2 = 130 M^{-1} Error = ± 5 %

Figure S39 ^{1}H NMR titration of compound **3** *vs.* TBABr in MeCN-d_3. Following the NH.

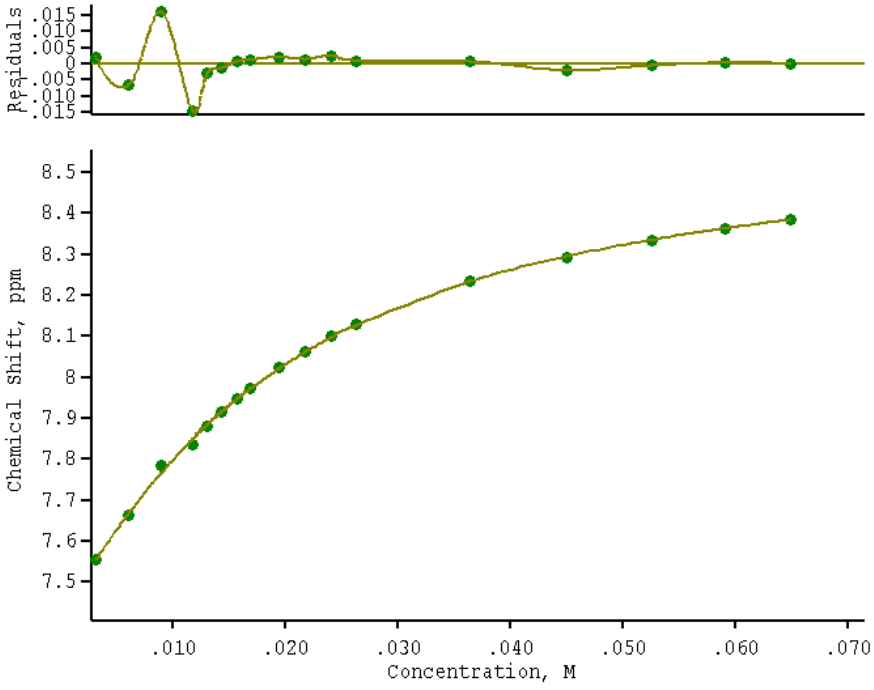

K_1 = 74 M^{-1} Error = ± 4 %

Figure S40 ^{1}H NMR titration of compound **3** *vs.* TBAI in MeCN-d_3. Following the NH.

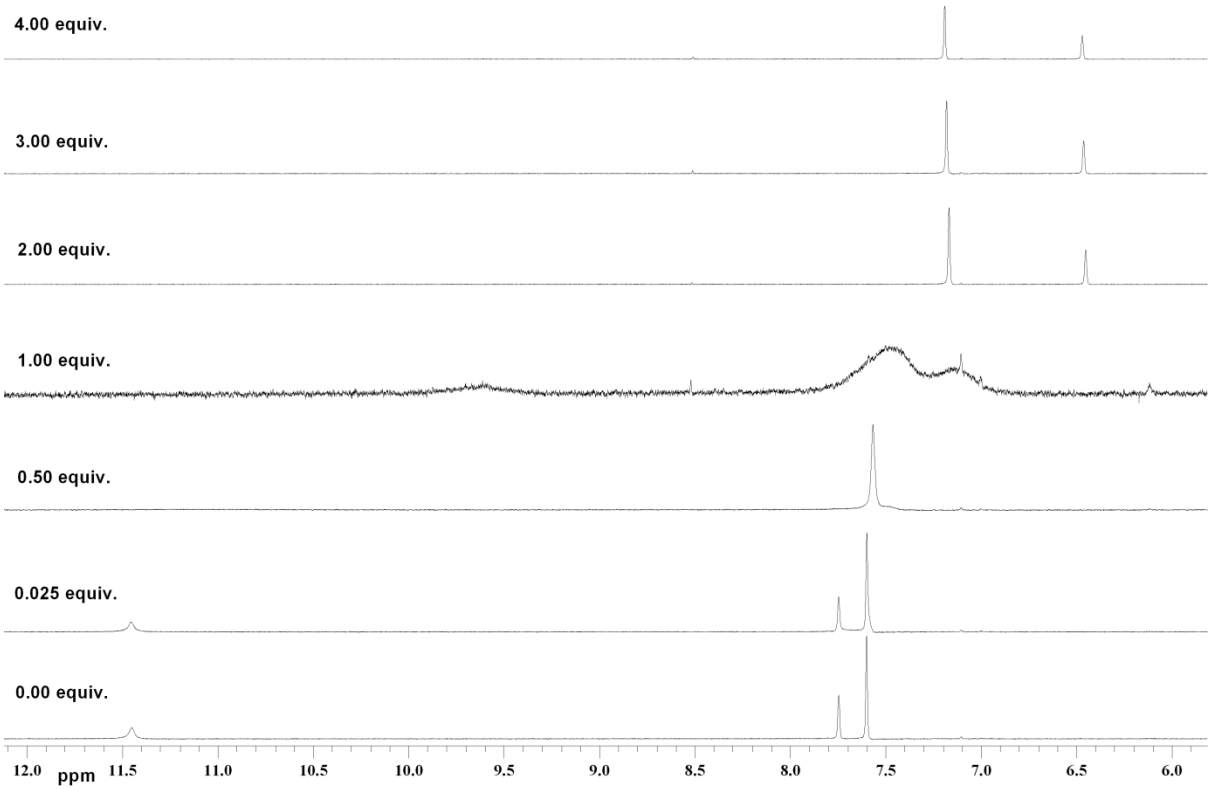

Figure S41 ^{1}H NMR stack plot of compound **1** *vs*. TBAOH in DMSO-d_6/H_2O 0.5%.

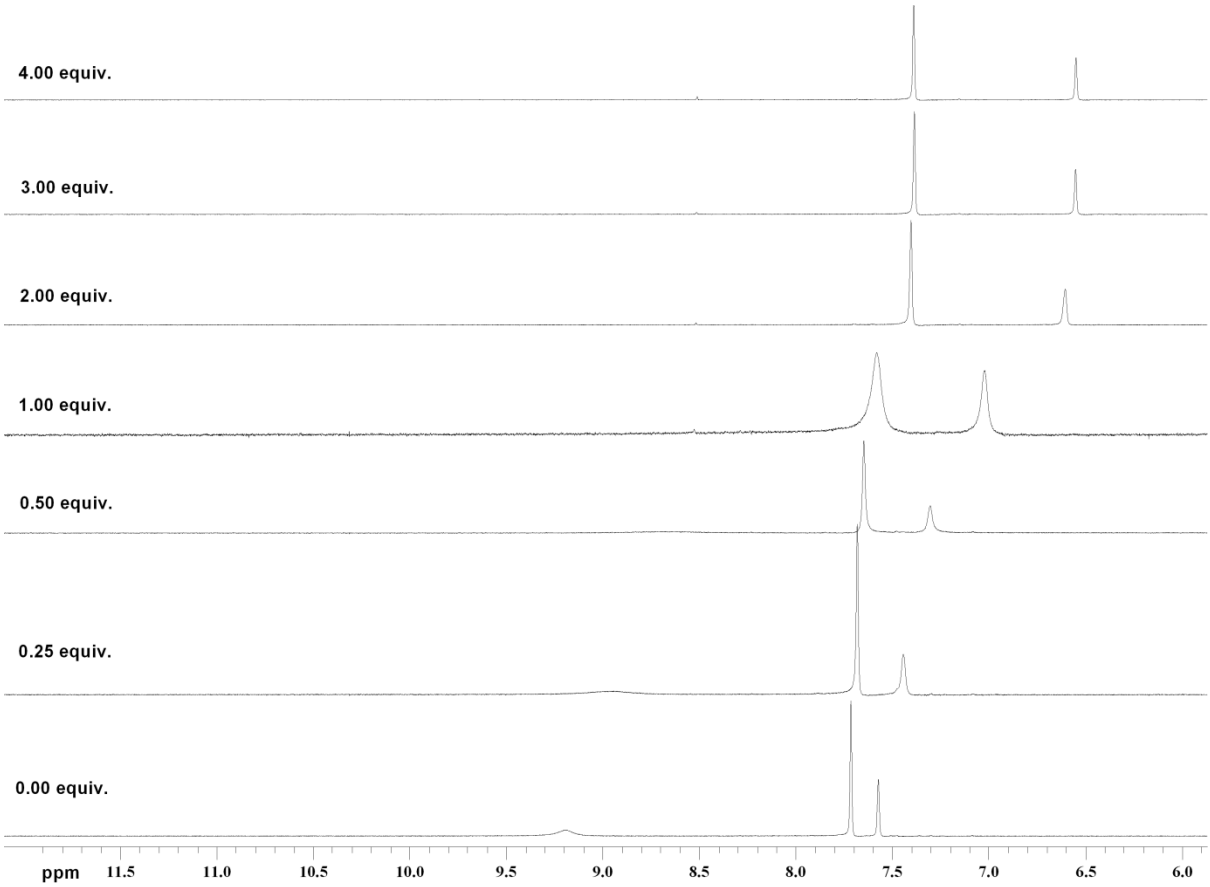

Figure S42 ^{1}H NMR stack plot of compound **2** *vs*. TBAOH in DMSO-d_6/H_2O 0.5%.

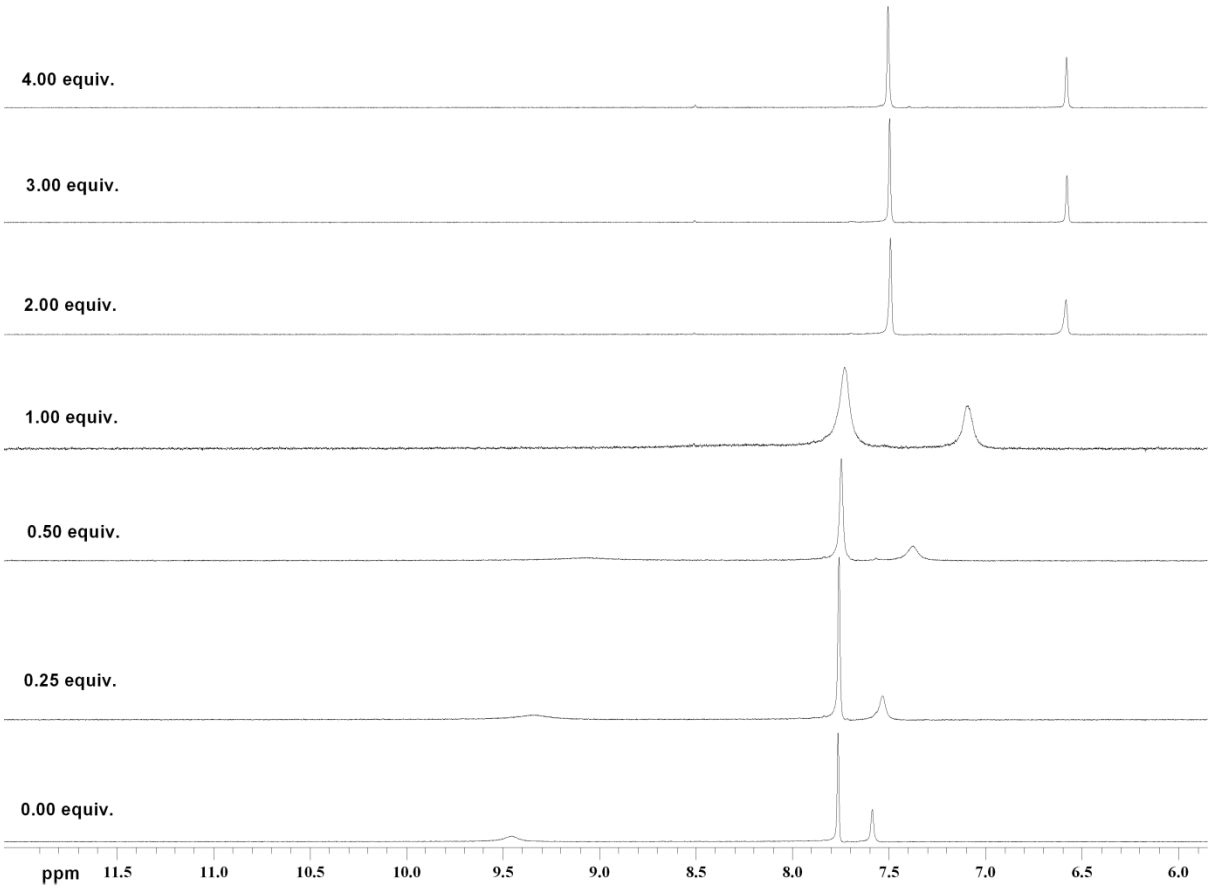

Figure S43 ^{1}H NMR stack plot of compound **3** *vs*. TBAOH in DMSO-d_6/H_2O 0.5%.

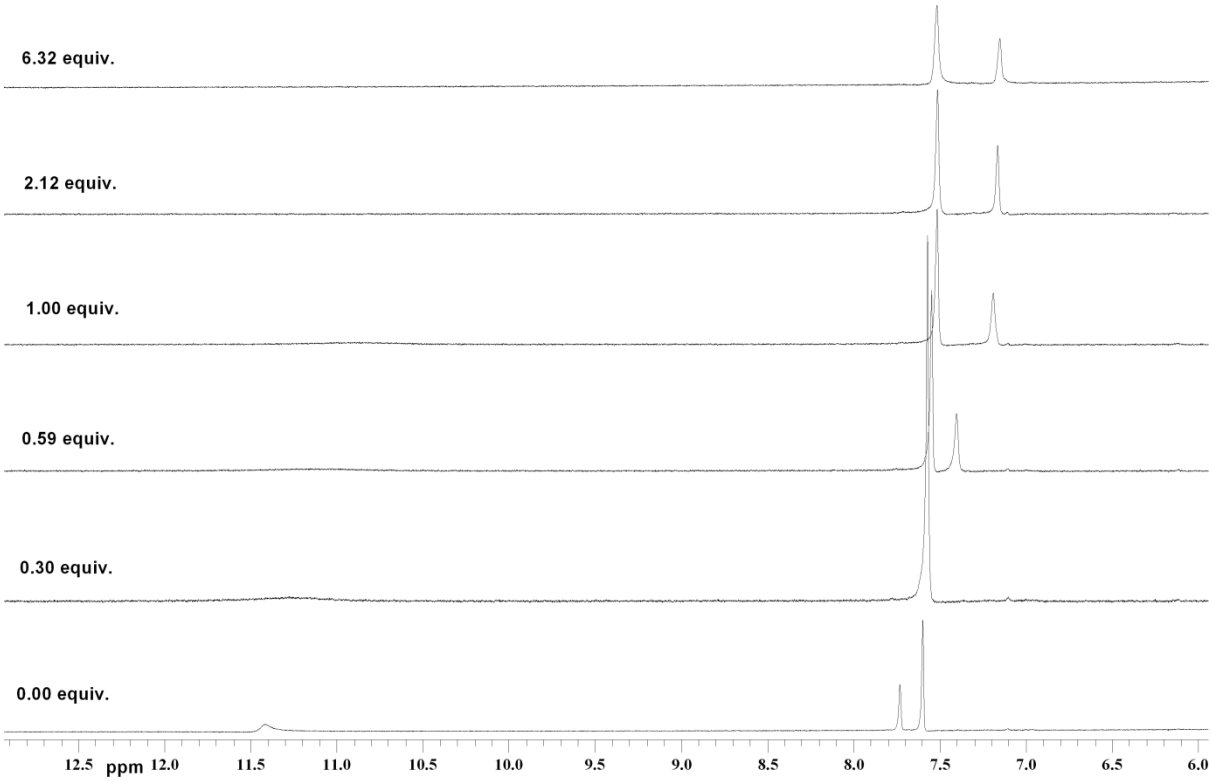

Figure S44 ^{1}H NMR stack plot of compound **1** *vs*. TBAOAc in DMSO-d_6/H_2O 0.5%.

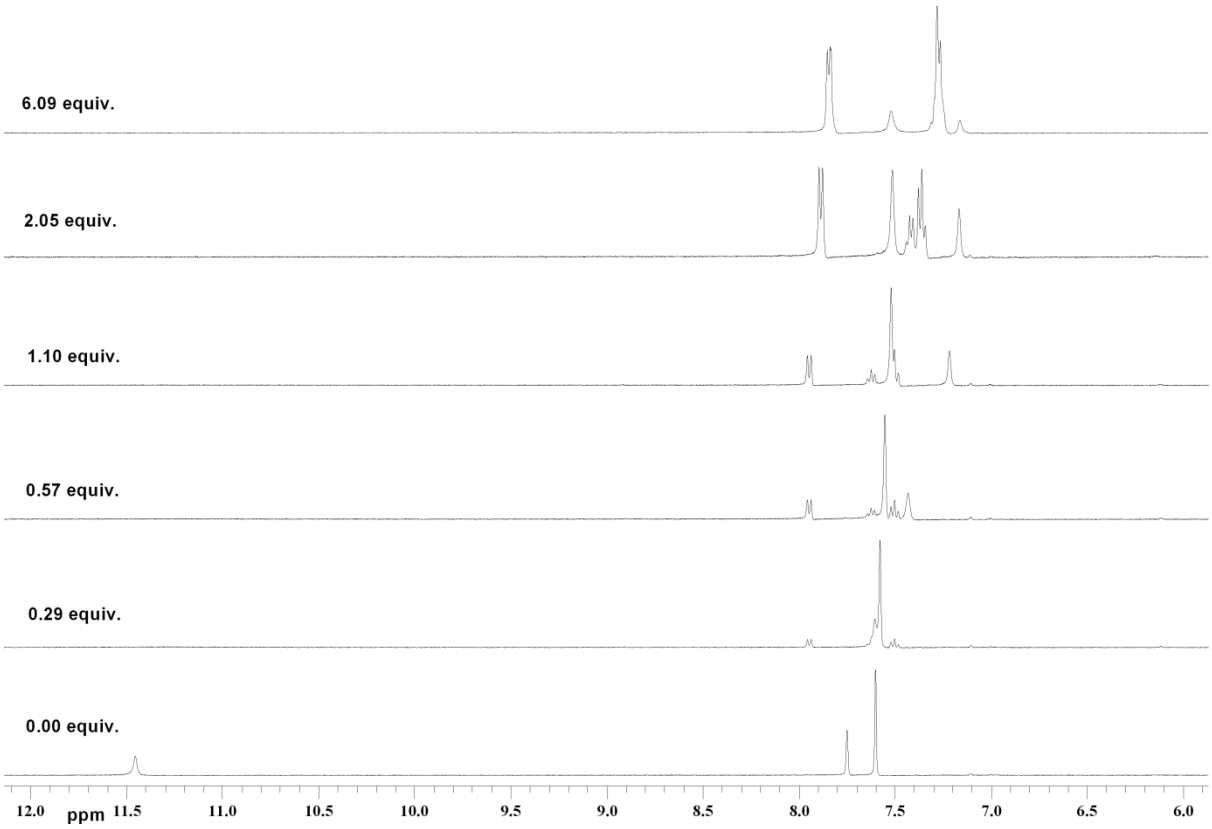

Figure S45 ^{1}H NMR stack plot of compound **1** *vs*. TBAOBz in DMSO-d_6/H_2O 0.5%.

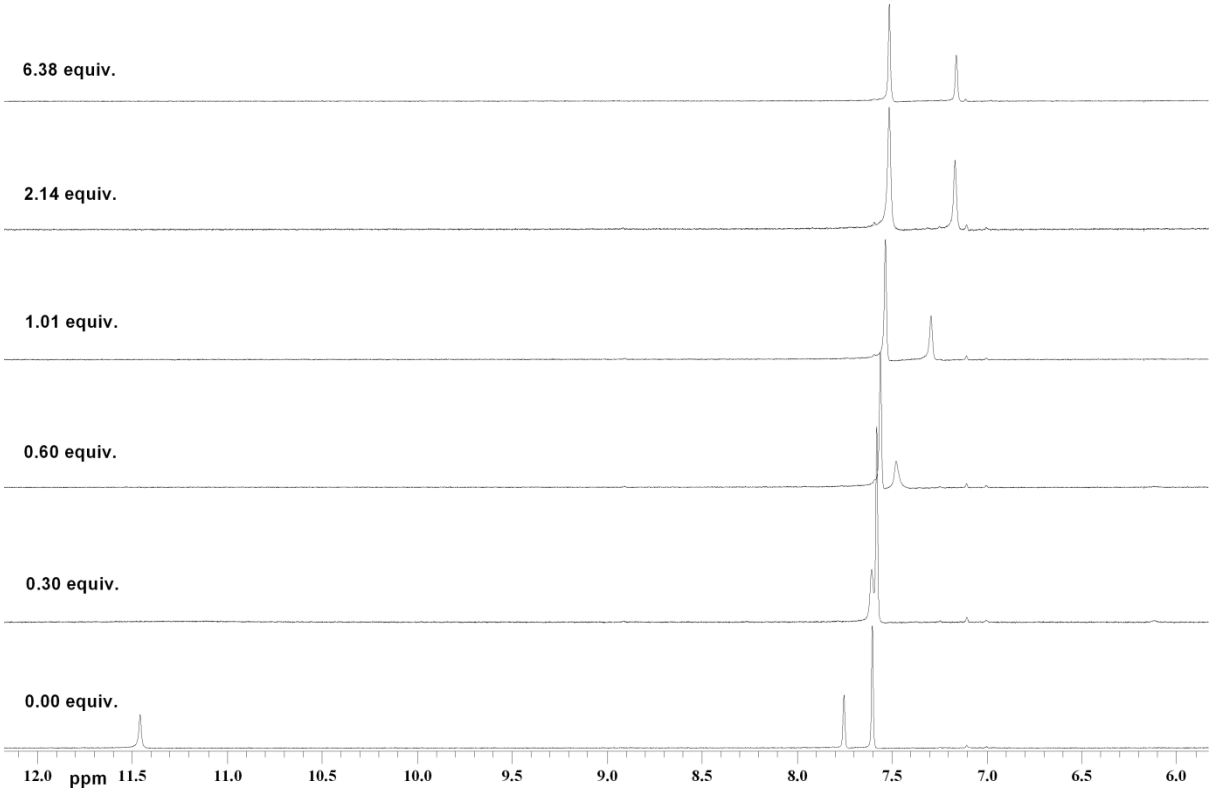

Figure S46 ^{1}H NMR stack plot of compound **1** *vs*. $TBAH_2PO_4$ in DMSO-d_6/H_2O 0.5%.

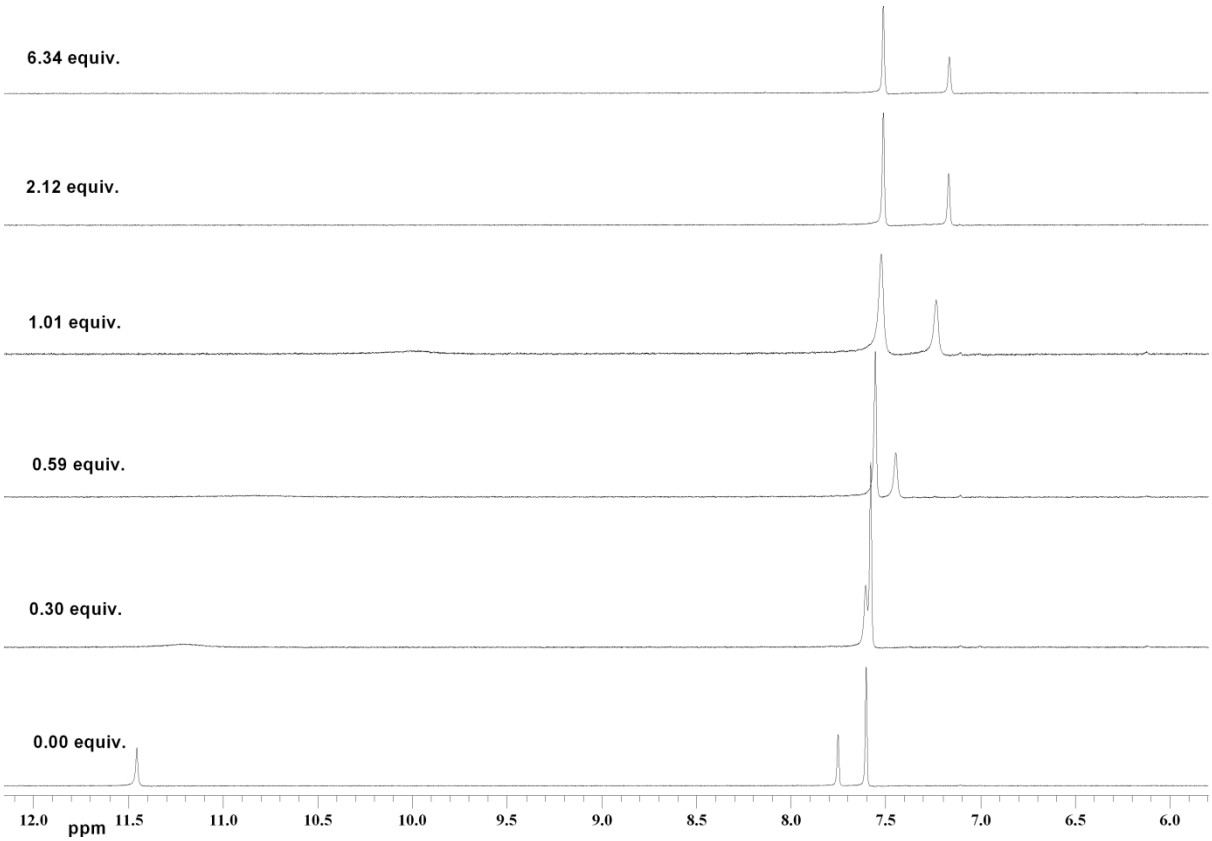

Figure S47 ^{1}H NMR stack plot of compound **1** *vs*. $TEAHCO_3$ in DMSO-d_6/H_2O 0.5%.

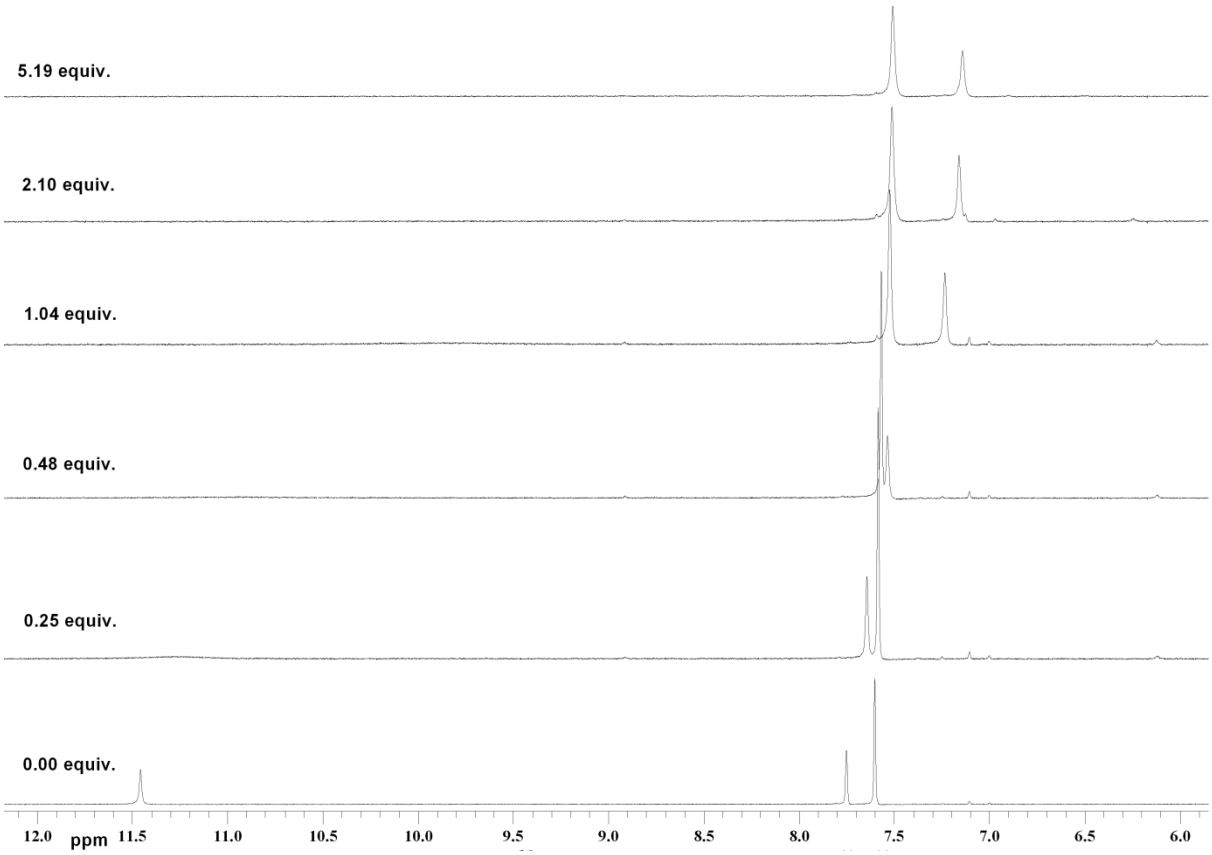

Figure S48 ^{1}H NMR stack plot of compound **1** *vs*. TBA_2SO_4 in DMSO-d_6/H_2O 0.5%.

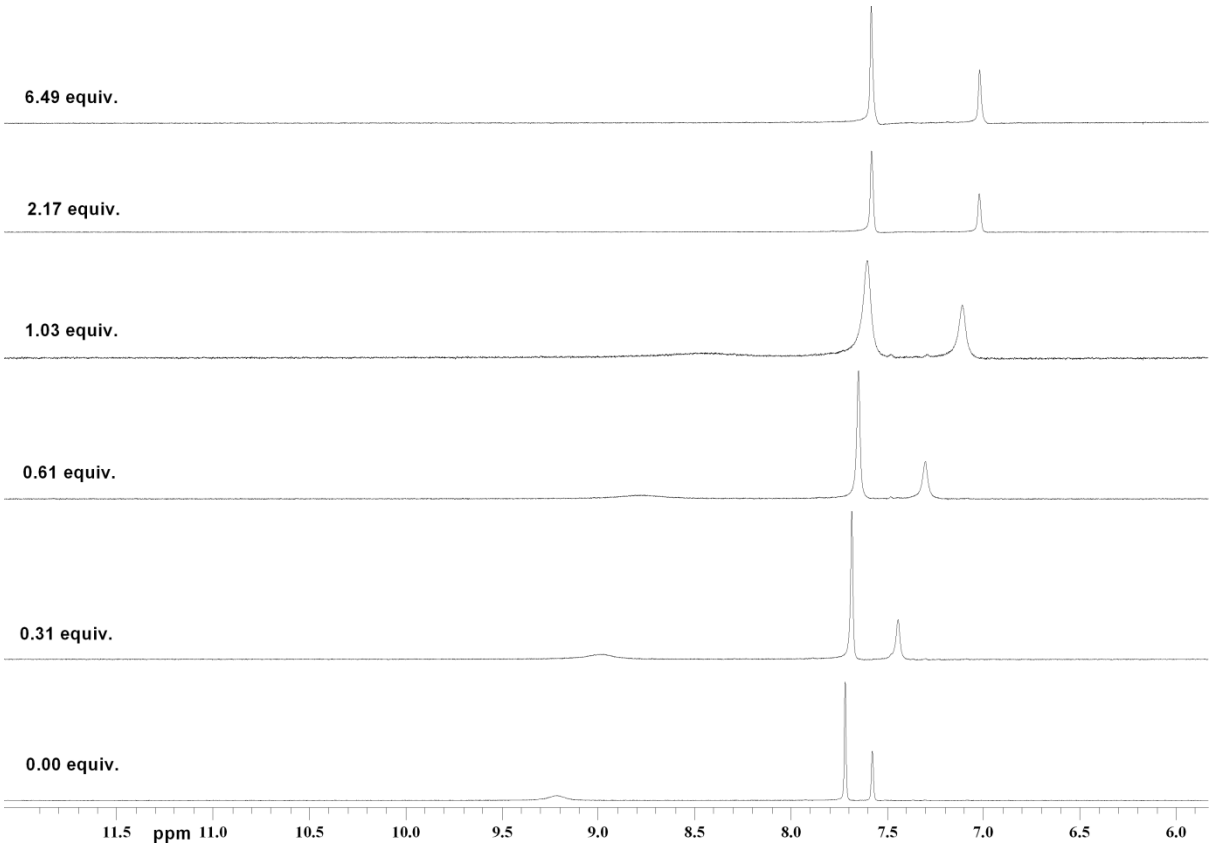

Figure S49 ^{1}H NMR stack plot of compound **2** *vs*. $TEAHCO_3$ in DMSO-d_6/H_2O 0.5%.

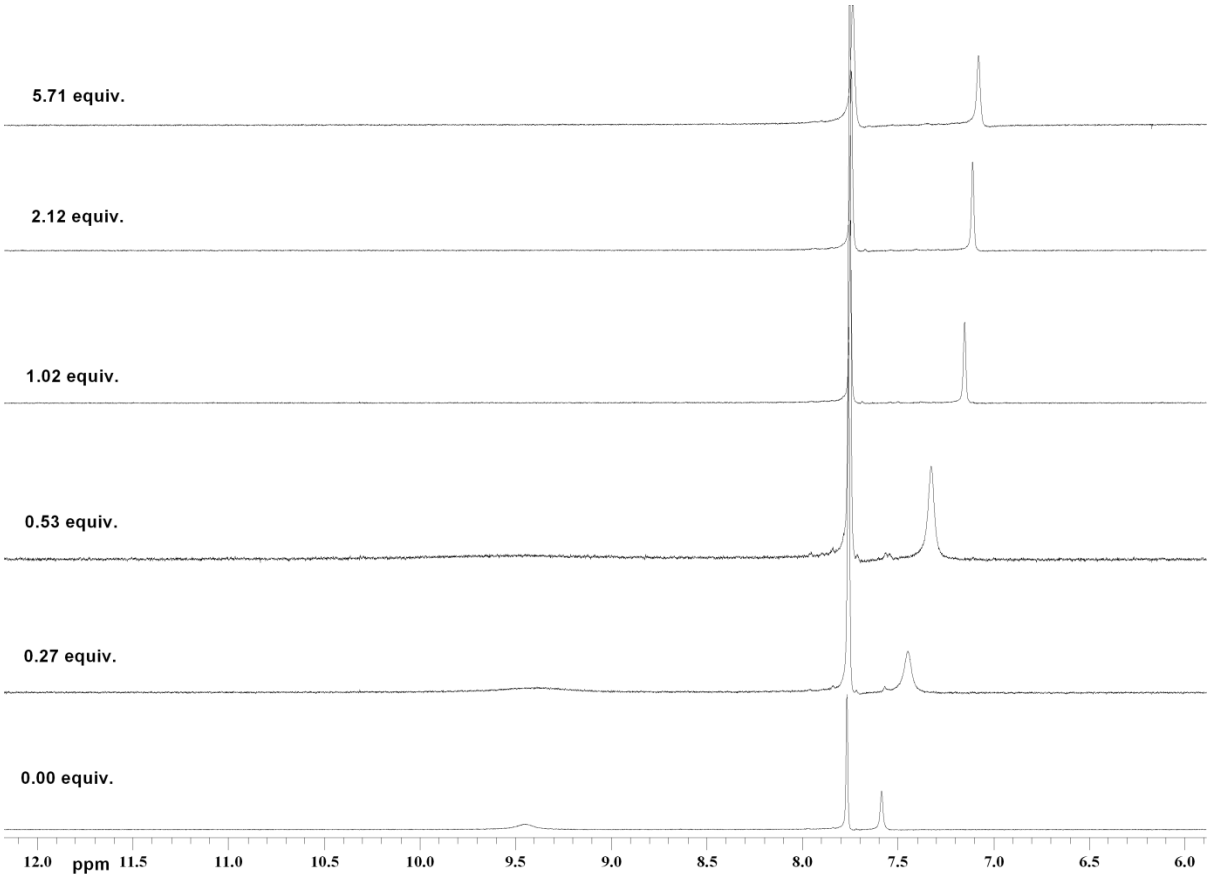

Figure S50 ^{1}H NMR stack plot of compound **3** *vs*. TBAOAc in DMSO-d_6/H_2O 0.5%.

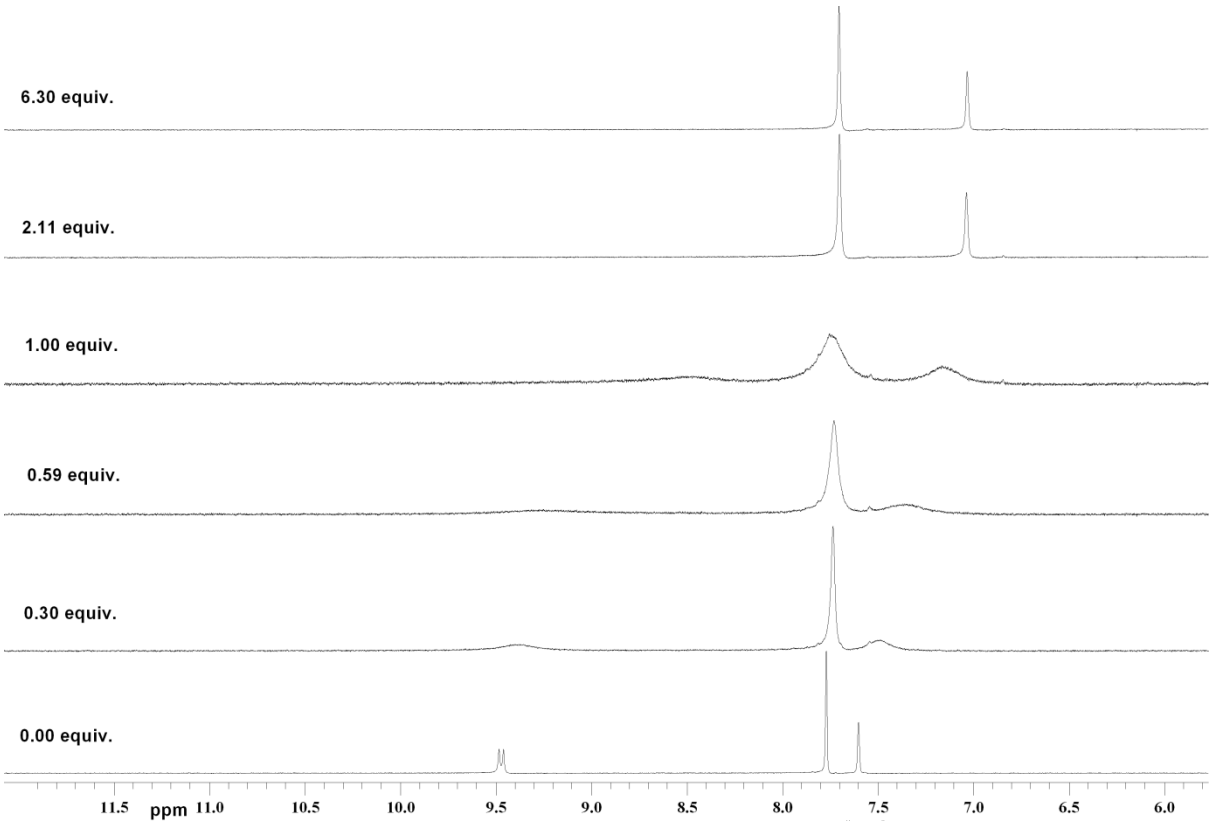

Figure S51 ^{1}H NMR stack plot of compound **3** *vs*. $TEAHCO_3$ in DMSO-d_6/H_2O 0.5%.

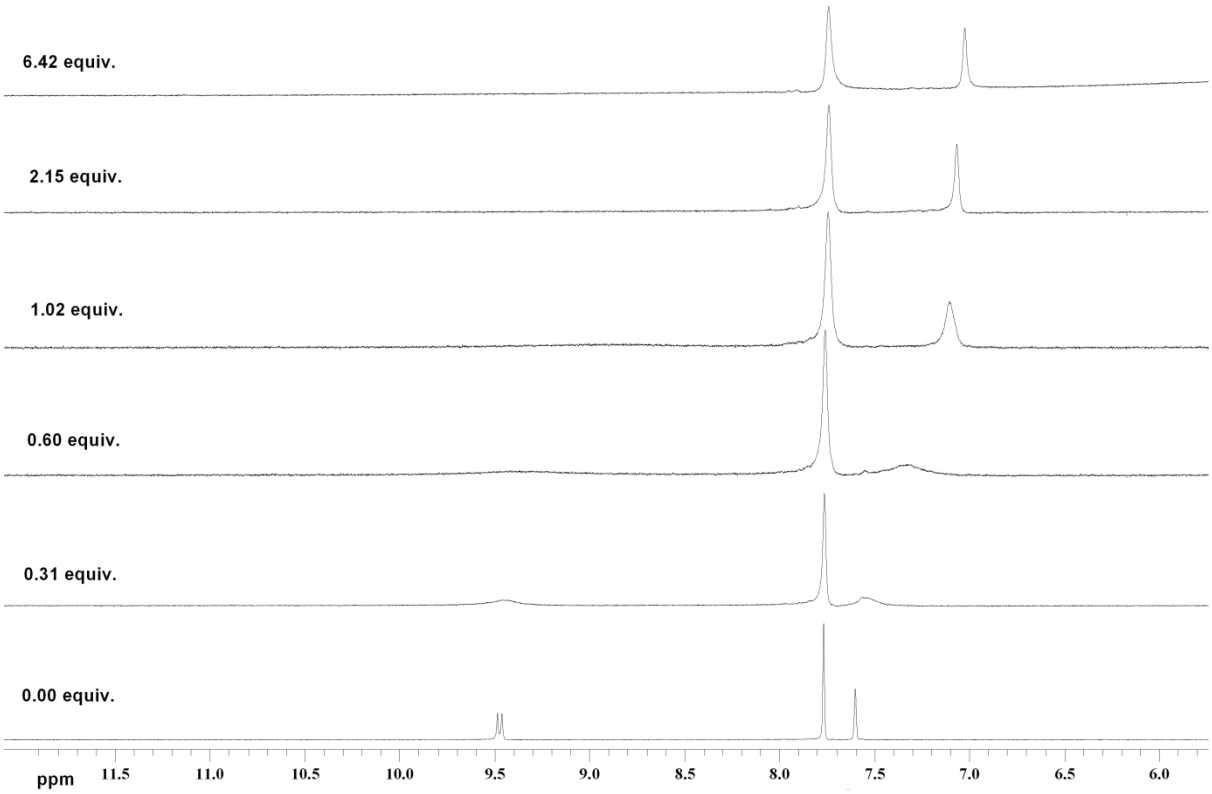

Figure S52 ^{1}H NMR stack plot of compound **3** *vs*. TBA_2SO_4 in DMSO-d_6/H_2O 0.5%.

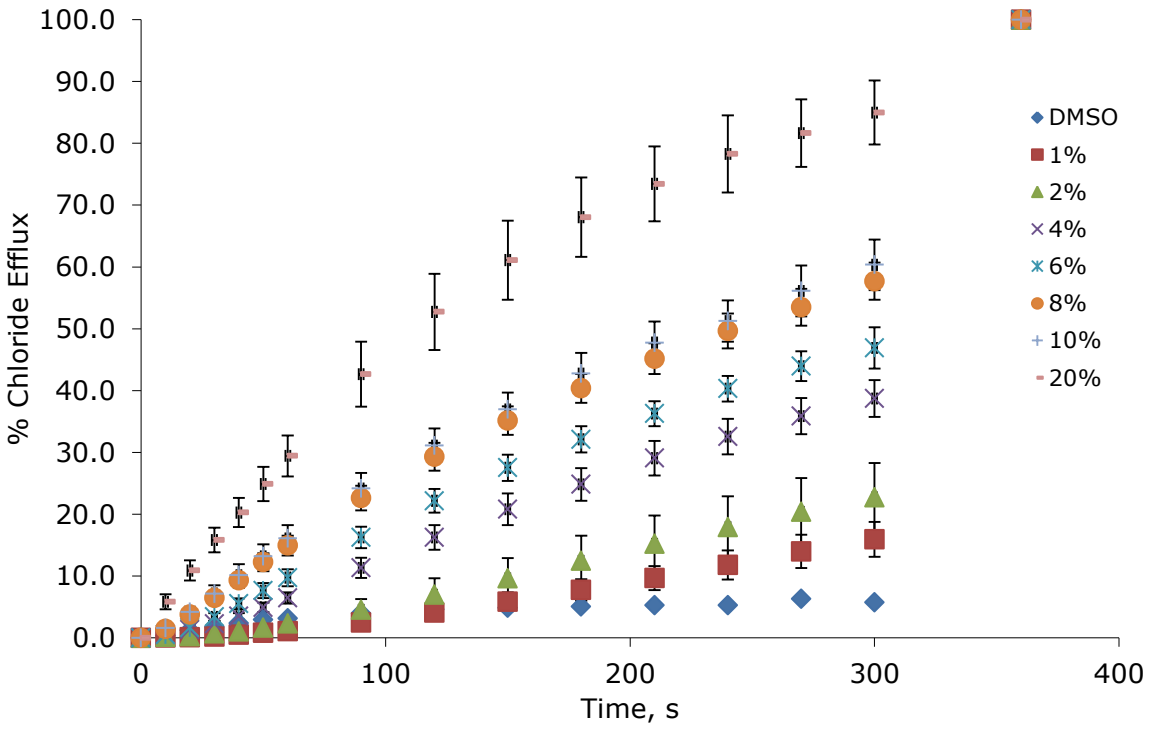

Figure S53 Chloride efflux promoted by a DMSO solution of compound **2** (various mol% carrier to lipid) from unilamellar POPC vesicles loaded with 488 mM NaCl buffered to pH 7.2 with 5 mM sodium phosphate salts. The vesicles were dispersed in 488 mM $NaNO_3$ buffered to pH 7.2 with 5mM sodium phosphate salts. At the end of the experiment detergent was added to lyse the vesicles and calibrate the ISE to 100% chloride efflux. Each point represents an average of three trials. DMSO was used as a control.

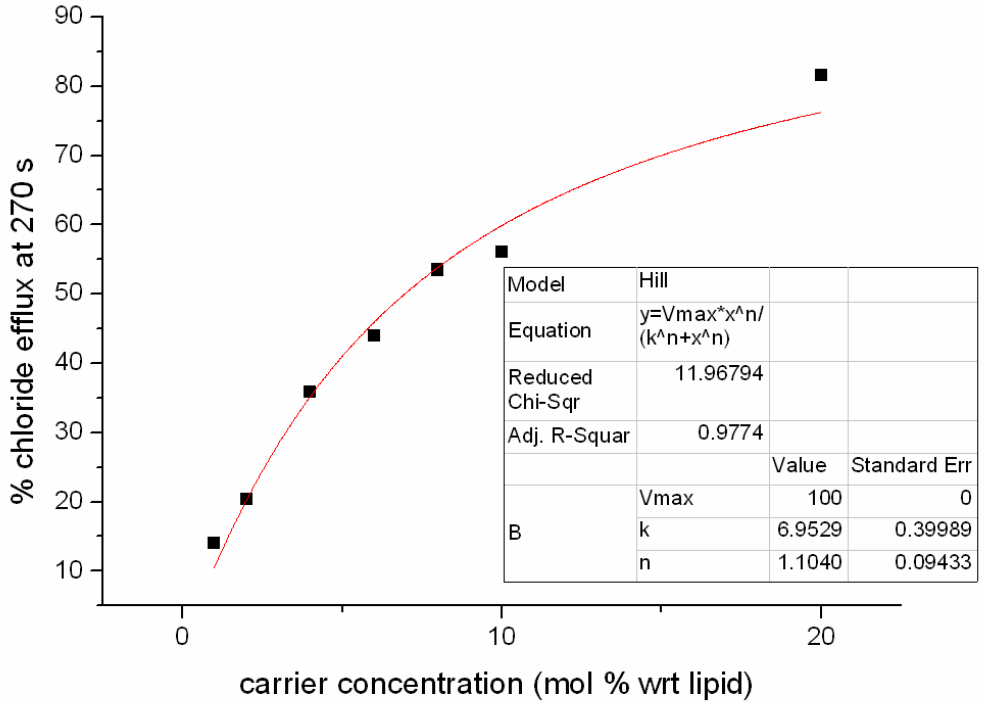

Figure S54 Hill plot for Cl^-/NO_3^- antiport by compound **2**.

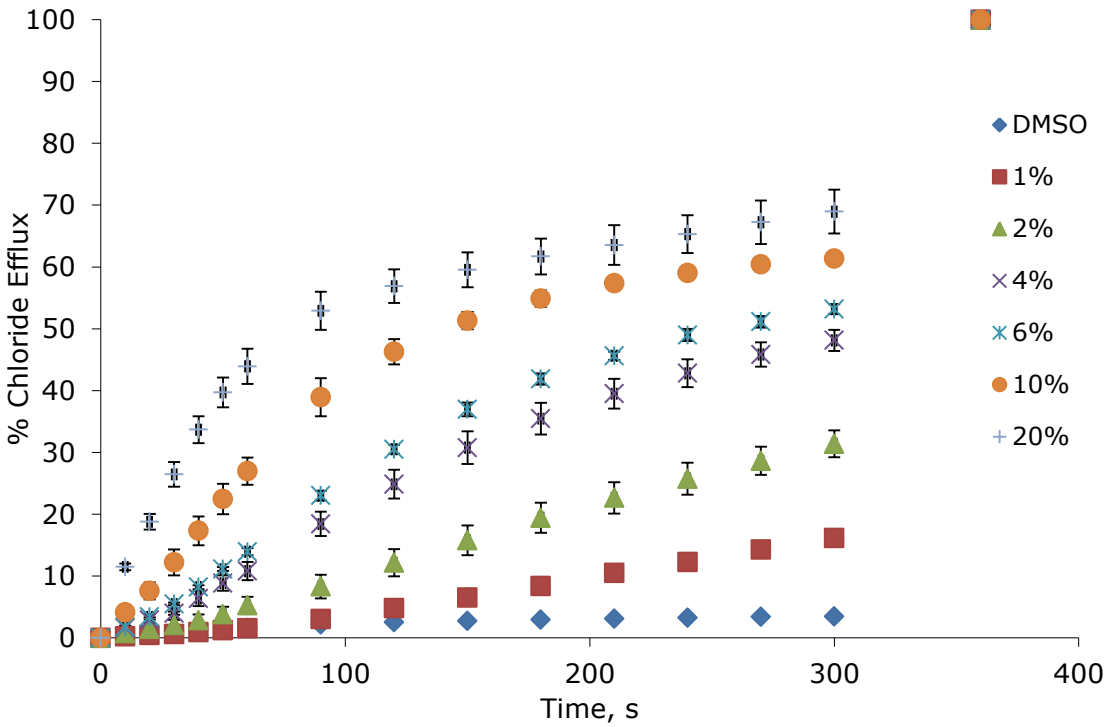

Figure S55 Chloride efflux promoted by a DMSO solution of compound **3** (various mol% carrier to lipid) from unilamellar POPC vesicles loaded with 488 mM NaCl buffered to pH 7.2 with 5 mM sodium phosphate salts. The vesicles were dispersed in 488 mM $NaNO_3$ buffered to pH 7.2 with 5mM sodium phosphate salts. At the end of the experiment detergent was added to lyse the vesicles and calibrate the ISE to 100% chloride efflux. Each point represents an average of three trials. DMSO was used as a control.

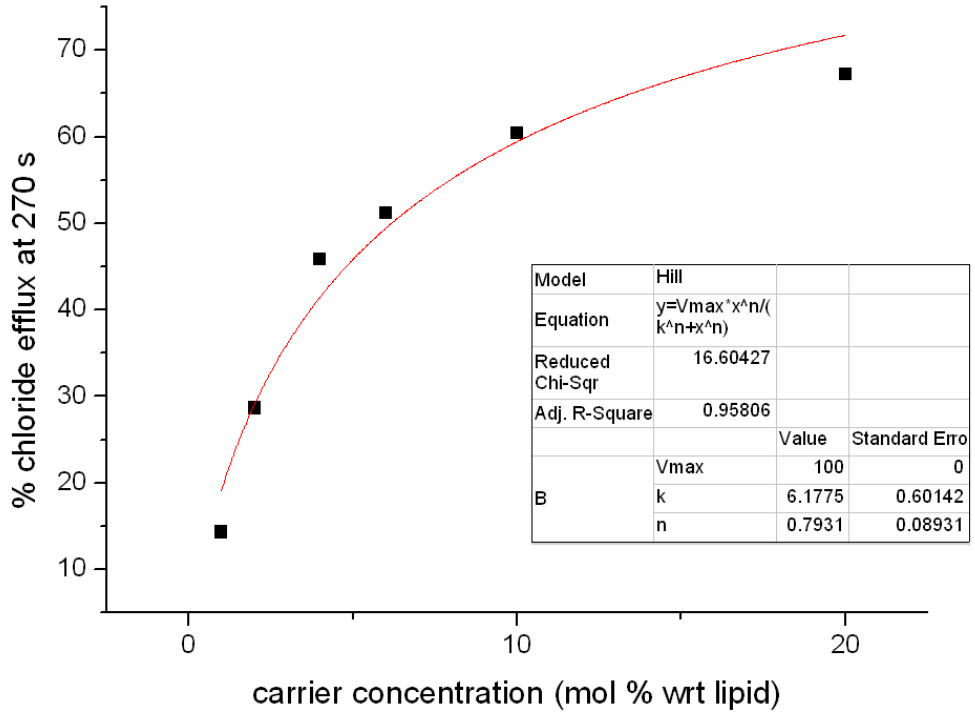

Figure S56 Hill plot for Cl^-/NO_3^- antiport by compound **3**.

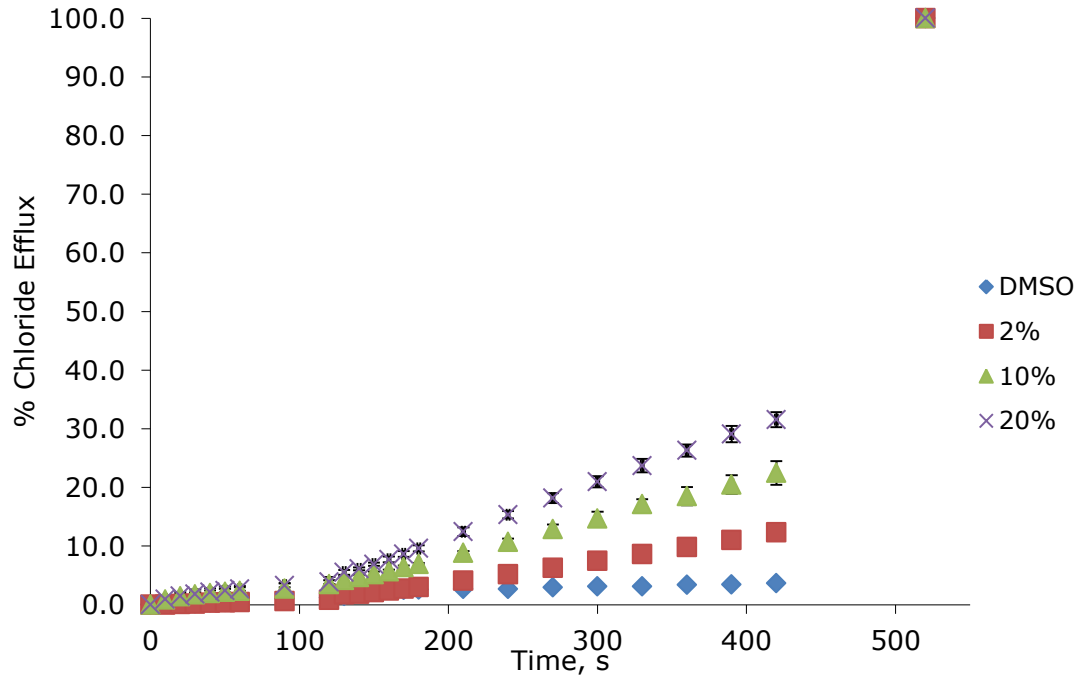

Figure S57 Chloride efflux promoted by a DMSO solution of compound **2** (various mol% carrier to lipid) from unilamellar POPC vesicles loaded with 451 mM NaCl buffered to pH 7.2 with 20 mM sodium phosphate salts. The vesicles were dispersed in 150 mM Na_2SO_4 buffered to pH 7.2 with 20 mM sodium phosphate salts. At t = 120 s a solution of sodium bicarbonate was added such that the external concentration of bicarbonate was 40 mM. At the end of the experiment, detergent was added to lyse the vesicles and calibrate the ISE to 100% chloride efflux. Each point represents an average of three trials. DMSO was used as a control.

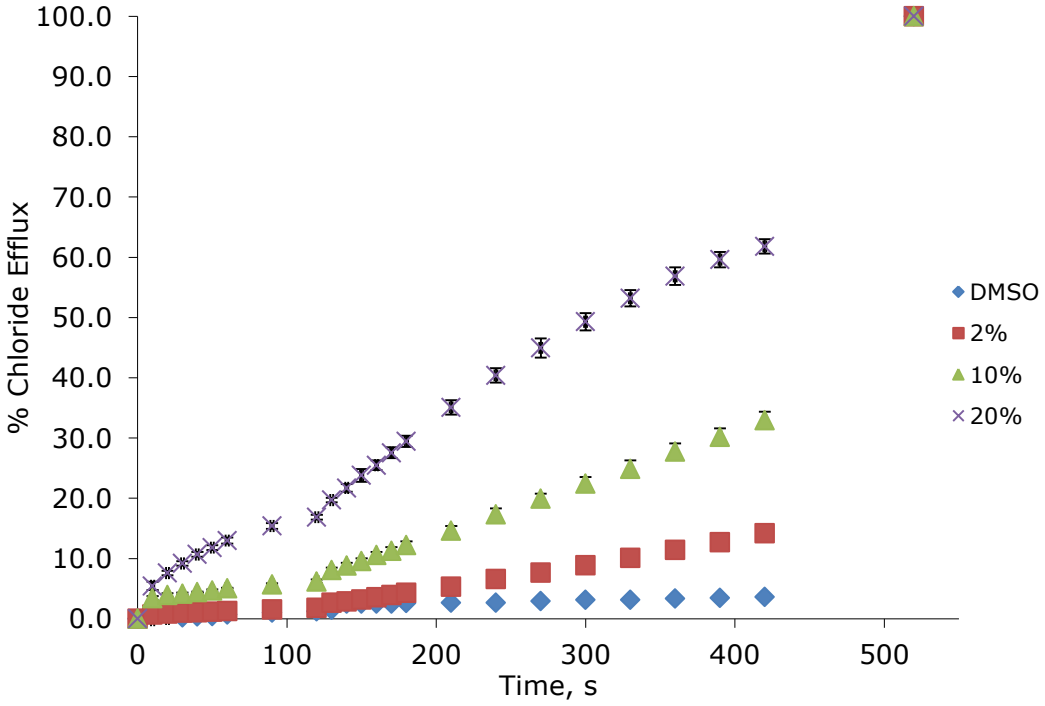

Figure S58 Chloride efflux promoted by a DMSO solution of compound **3** (various mol% carrier to lipid) from unilamellar POPC vesicles loaded with 451 mM NaCl buffered to pH 7.2 with 20 mM sodium phosphate salts. The vesicles were dispersed in 150 mM Na_2SO_4 buffered to pH 7.2 with 20 mM sodium phosphate salts. At t = 120 s a solution of sodium bicarbonate was added such that the external concentration of bicarbonate was 40 mM. At the end of the experiment, detergent was added to lyse the vesicles and calibrate the ISE to 100% chloride efflux. Each point represents an average of three trials. DMSO was used as a control.

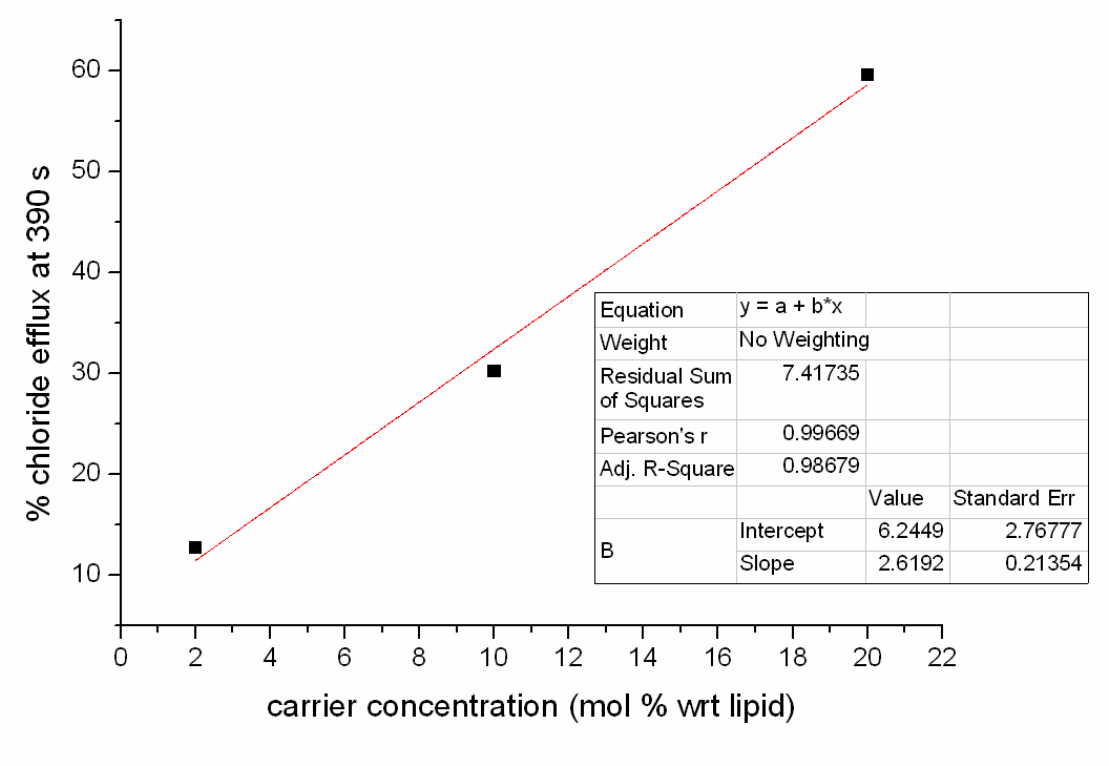

Figure S59 Attempted EC_{50} determination for Cl-/HCO3- antiport by compound **3**. Due to poor activity the data was fitted to a straight line with the approximate EC_{50} = 16.7 %.

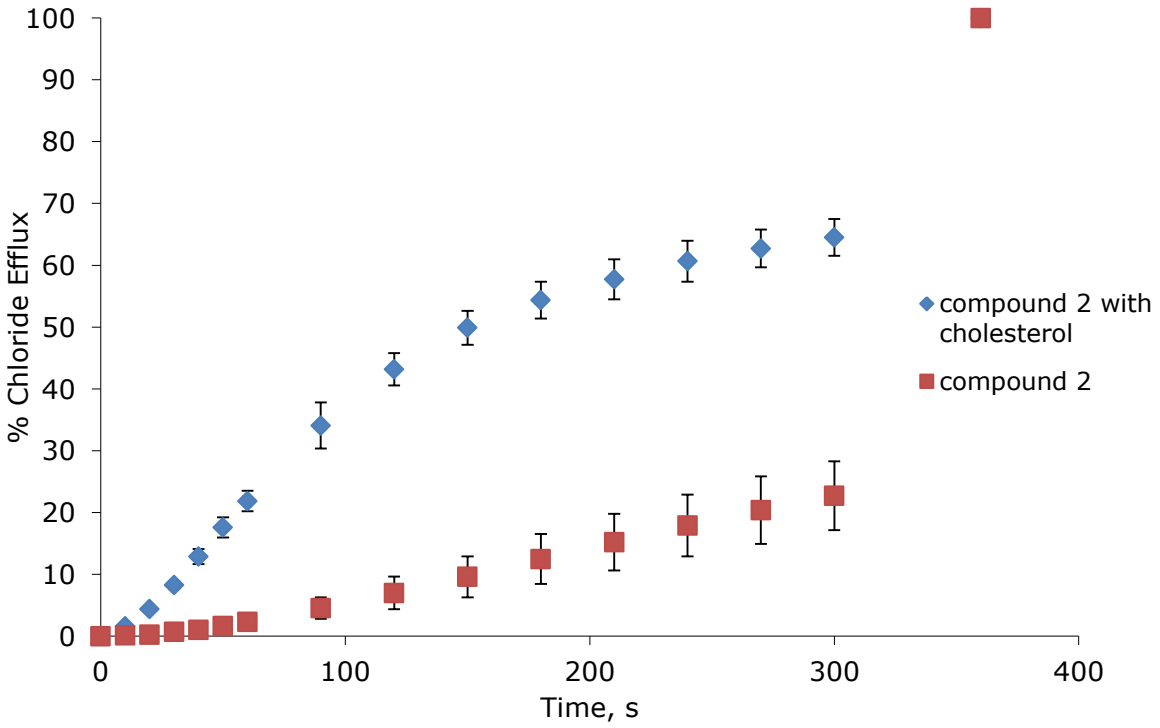

Figure S60 Chloride efflux promoted by a DMSO solution of compound **2** (2 mol% carrier to lipid) from unilamellar vesicles composed of POPC/cholesterol (7:3) loaded with 488 mM NaCl buffered to pH 7.2 with 5 mM sodium phosphate salts. The vesicles were dispersed in 488 mM $NaNO_3$ buffered to pH 7.2 with 5mM sodium phosphate salts. At the end of the experiment detergent was added to lyse the vesicles and calibrate the ISE to 100% chloride efflux. Each point represents an average of three trials. DMSO was used as a control.

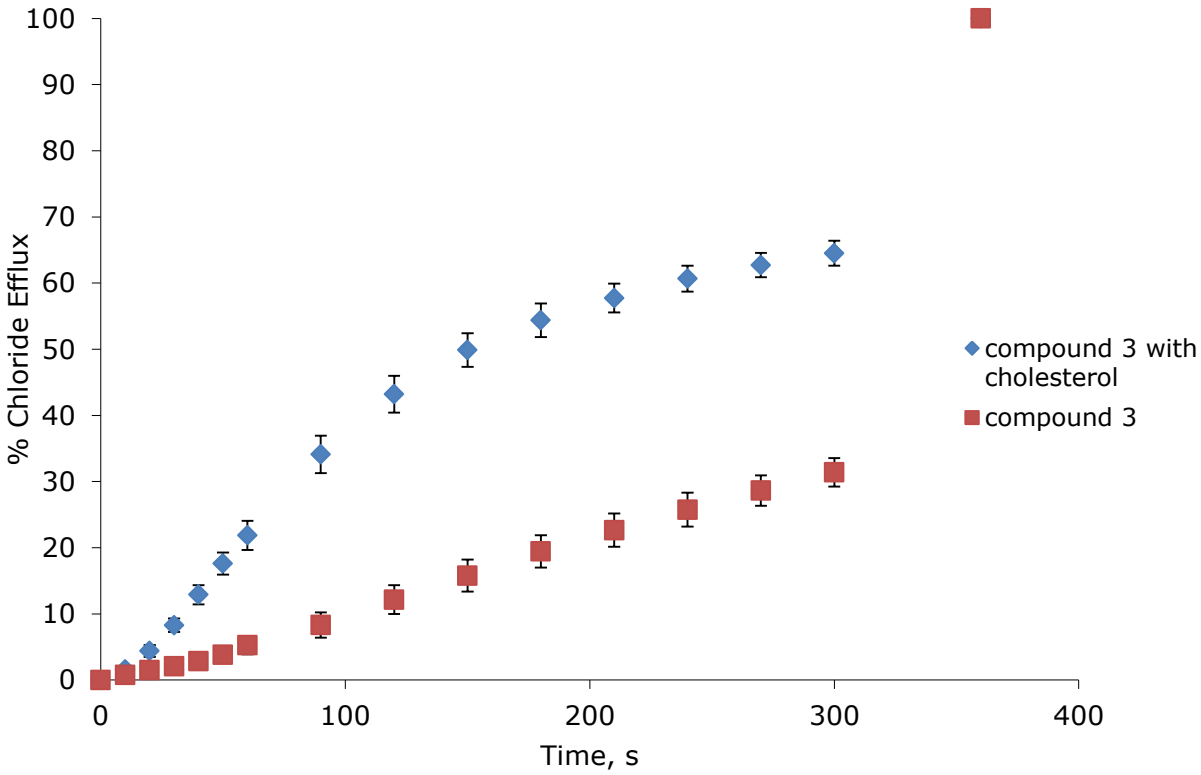

Figure S61 Chloride efflux promoted by a DMSO solution of compound **3** (2 mol% carrier to lipid) from unilamellar vesicles composed of POPC/cholesterol (7:3) loaded with 488 mM NaCl buffered to pH 7.2 with 5 mM sodium phosphate salts. The vesicles were dispersed in 488 mM $NaNO_3$ buffered to pH 7.2 with 5mM sodium phosphate salts. At the end of the experiment detergent was added to lyse the vesicles and calibrate the ISE to 100% chloride efflux. Each point represents an average of three trials. DMSO was used as a control.

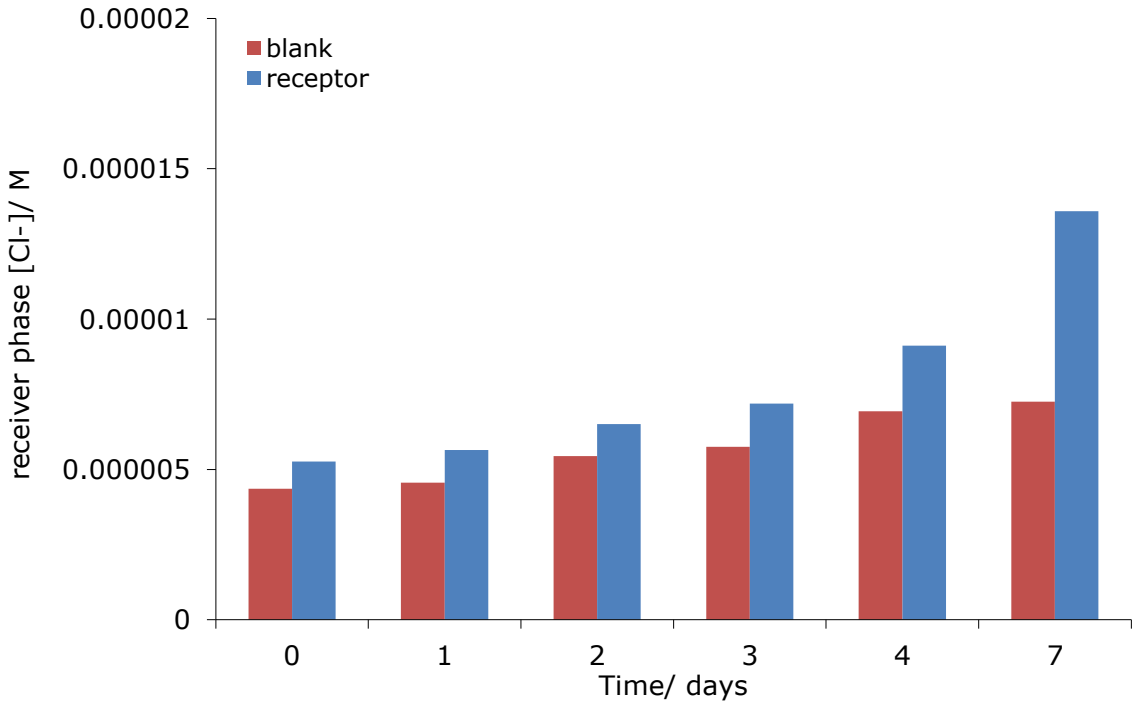

Figure S62 Chloride concentration of the receiver phase (initial composition 489 mM $NaNO_3$ buffered to pH 7.2 with 5 mM sodium phosphate salts) in a U-tube mobility assay with compound **3.**

Figure S63 DMSO solutions of compound **1** with (left to right; TBAI, TBABr, TBACl, $TBANO_3$, $TBAHSO_4$, $TBAH_2PO_4$, TBAOBz, TBAOAc, $TEAHCO_3$, TBA_2SO_4 and TBAOH.

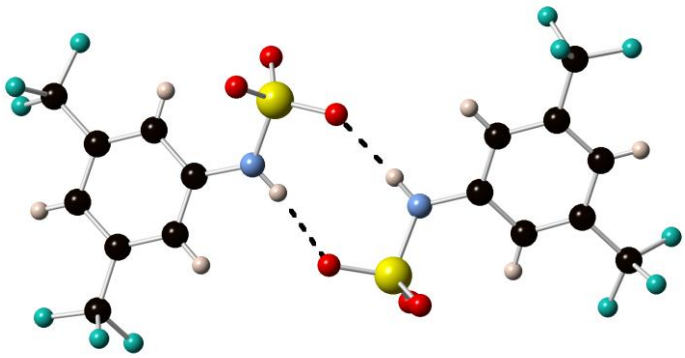

Figure S64 The X-ray crystal structure of a dimer of the decomposition products for compound **1**. The tetrabutylammonium counterions have been removed for clarity.

Table S1 Hydrogen bonding lengths and angles for the crystal structure of the decomposition products for compound **1**.

Atom D	Atom H	Atom A	DH distance/ Å	HA distance/ Å	DA distance/ Å	DHA angle/ °
N7	H7	O6	0.86	2.06	2.833(7)	149.8
N6	H6	O2	0.86	2.08	2.891(7)	156.1

References

1. A. A. Rodriguez, H. Yoo, J. W. Ziller, K. J. Shea, *Tet. Lett.*, **2009**, *50*, 6830-6833.